Journal of Medicinal Chemistry

Article

Discovery of intestinal targeted TGR5 agonists for the treatment of type 2 diabetes

hongliang duan, mengmeng ning, qingan zou, yangliang ye, ying feng, lina zhang, Ying Leng, and Jianhua Shen

J. Med. Chem., **Just Accepted Manuscript** • DOI: 10.1021/jm500829b • Publication Date (Web): 24 Feb 2015

Just Accepted

Journal of Medicinal Chemistry is published by the American Chemical Society. 1155 Sixteenth Street N.W., Washington, DC 20036

Discovery of intestinal targeted TGR5 agonists for the treatment of type 2 diabetes

Hongliang Duan,† Mengmeng Ning,† Qingan Zou, Yangliang Ye, Ying Feng, Lina Zhang, Ying Leng, Jianhua Shen**

State Key Laboratory of Drug Research, Shanghai Institute of Materia Medica (SIMM), Chinese Academy of Sciences, Shanghai 201203, China

ABSTRACT

Activation of TGR5 stimulates intestinal glucagon-like peptide-1 (GLP-1) release, but activation of the receptors in gallbladder and heart has been shown to cause severe on target side effects. A series of low-absorbed TGR5 agonists was prepared by modifying compound **2** with polar functional groups to limit systemic exposure and specifically activate TGR5 in the intestine. Compound **15c**, with a molecular weight of 1401, a PSA value of 223 $Å^2$, and low permeability on Caco-2 cells, exhibited satisfactory potency both *in vitro* and *in vivo*. Low levels of **15c** were detected in blood, bile, and gallbladder tissue, and gallbladder related side effects were substantially decreased compared to the absorbed small-molecule TGR5 agonist **2**.

INTRODUCTION

TGR5 (GPBAR1, M-BAR, GPCR19) is a G protein-coupled receptor (GPCR) first identified as a cell-surface bile acid receptor in 2002.[1] Activation of TGR5 promotes secretion of glucagon-like peptide-1 (GLP-1),[2] which activates insulin secretion, suppresses glucagon release as well as

slows gastric emptying and suppresses appetite.[3,4] Elevated GLP-1 concentrations increase glucose disposal and decrease blood glucose levels. In addition, TGR5 involves in metabolic regulation in brown fat and skeletal muscle during energy expenditure.[5,6] Since obesity and weight gain are common complications in type 2 diabetes mellitus (T2DM), TGR5 agonists may provide new treatments forT2DM and associated metabolic diseases.[7,8,9]

Human TGR5 shares 83% amino acid sequence identity with TGR5 in mice.[10] TGR5 gene expression is widely distributed, with moderate expression levels in the intestine, spleen, and placenta, and greater expression level in the gallbladder.[11,12] Activation of TGR5 in gallbladder epithelium causes smooth muscle relaxation, stimulation of gallbladder filling, and an acute increase in gallbladder volume.[13] TGR5 agonists also produce cardiovascular effects, such as changes in heart rate.[14,15] The gallbladder and cardiac side effects are the main obstacles to the clinical application of TGR5 agonists.

There are two categories of TGR5 agonists at present. The first series includes naturally occurring bile acids (BAs) such as cholic acid (CA) and lithocholic acid (LCA),[1] and their semisynthetic derivatives such as 6α-ethyl-23(S)-methylcholic acid (INT777, **1**, Figure **1**),[16] while the second series consists of synthetic small molecules.[17-23] We previously reported a series of orally efficacious TGR5 agonists based on 4-phenoxynicotinamide, of which one of the most potent molecules was [4-(2,5-dichlorophenoxy)-pyridin-3-yl]-(4-cyclopropyl-3,4-dihydro-2*H*-quinoxalin-1-yl)-methanone (**2**, Figure **1**).[24] These agonists exhibited nanomolar potency and were proved to be effective in lowering glucose levels following an oral administration. High exposure to intestine caused the secretion of GLP-1, but exposure to other tissues such as gallbladder and heart resulted in unwanted side effects.[24] It was well reported that the volume of the gallbladder would increase after oral administration of TGR5 agonists.[13] To minimize the

side effects, developing non-systemic TGR5 agonists specially targeting intestinal system became our strategy.

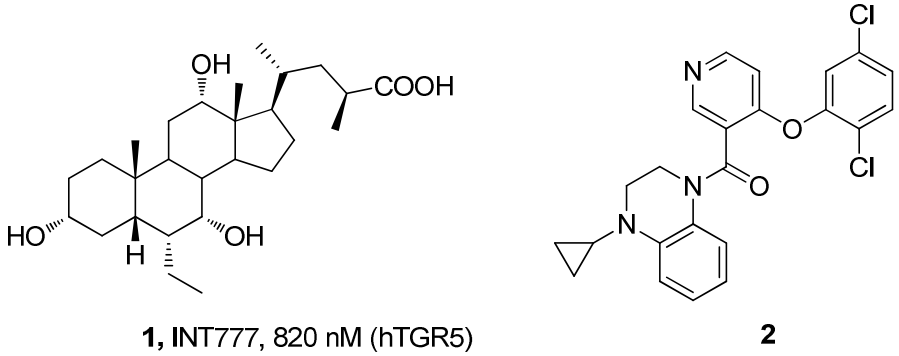

1, INT777, 820 nM (hTGR5) **2**

Figure 1. Structures of some TGR5 agonists.

Since TGR5 is expressed in the intestinal tract[11] and GLP-1 is an intestinal peptide secreted from colonic L cells as well,[25] localized stimulation of TGR5 within the colon to initiate GLP-1 release is possible.[9] This hypothesis is also supported by an *ex vivo* explant study that TGR5 agonists induces GLP-1 secretion in the explanted intestinal tract.[26] Therefore, for the TGR5 agonists, the absorption from the intestine to the plasma may be not necessary to activate intestinal TGR5 receptors, stimulate secretion of GLP-1, and provide the desired antidiabetic effect. Non-absorbed molecular therapeutics are usually developed to interact with intestinal targets selectively, minimize off-target systemic effects, and reduce toxicity and side-effects.[27] There are several other non-absorbed antidiabetic agents including the α-glucosidase inhibitor acarbose,[28] the apical sodium-dependent bile acid transporter (ASBT) inhibitor 3-({[(3R,5R)-3-butyl-3-ethyl-7-(methyloxy)-1,1-dioxido-5-phenyl-2,3,4,5-tetrahydro-1,4-benzothiazepin-8-yl]methyl}-amino)pentanedioic acid (GSK2330672),[29] and the non-systemic TGR5 agonists developed by Exelixis, Inc.[30] and Ardelyx, Inc..[31] We focus our investigations on non-absorbed TGR5 agonists with the expectation that these compounds would exert their therapeutic effects

locally in the gastrointestinal (GI) tract rather than in the gallbladder.

We sought to develop a series of non-absorbed TGR5 agonists by incorporating hydrophilic groups on to the previously described series to reduce intestinal permeability and restrict activation of TGR5 to the intestine.[32] In our previous study of 4-phenoxynicotinamide derivatives as TGR5 agonists, a wide range of functional groups including chlorine, bromine, methyl, and ethyl were well tolerated at 4-position of the phenoxy moiety, suggesting that this position may fit into a large pocket within the TGR5 receptor (Figure **1**).[24] We hypothesized that hydrophilic groups such as amino acids and PEG chains could be incorporated at this position to minimize systemic exposure while maintaining potency.

The polar surface area (PSA) correlates well with passive molecular transport throuth membranes and is an effective approach for predicting drug absorption in the GI tract (the Egan Egg model).[33] It incorporates most of Lipinski's "rule of 5" for oral bioavailability, including molecular weight, the number of hydrogen bond acceptors and donors within the compound.[27,32] Drugs with a PSA < 60 $Å^2$ are often completely absorbed from the intestine, while drugs with a PSA > 140 $Å^2$ are usually poorly absorbed.[34,35] In this report, the calculated PSA was employed as a predictive parameter to evaluate the gut permeability of TGR5 agonists, and our aim was to synthesize analogues well outside the normal range for orally bioavailable drugs, e.g. > 140 $Å^2$ PSA.

CHEMISTRY

Our routes for synthesizing amino acid or PEG containing derivatives of **2** are summarized in Schemes **1**-**3**. The key intermediate 4-bromophenoxy derivative **6** was synthesized from the commercially available 4-chloronicotinic acid as previously reported by our group.[24] As shown in Scheme **1**, 4-chloronicotinic acid was converted into the acyl chloride by treatment with

oxalyl chloride, followed by reaction with ethanol to afford the ester **3**. Treatment of intermediate **3** with 4-bromo-2,5-dichlorophenol in the presence of potassium carbonate yielded ester **4**, and subsequent hydrolysis of ester **4** provided acid **5**. The aryl bromide intermediate **6** was obtained by coupling of acid **5** with 1-cyclopropyl-1,2,3,4-tetrahydroquinoxaline. Heck reaction of aryl bromide **6** with ethyl acrylate generated the desired intermediate **7**.[20] Reduction of the double bond of olefin **7** with sodium borohydride in the presence of cuprous chloride gave compound **8**. A subsequent hydrolysis with sodium hydroxide yielded the acid **9**. This acid was coupled with a series of amino acid esters using HATU as a coupling reagent to produce the desired compounds **10a-c**. Compouds **10d-f** were obtained by hydrolysis of esters **10a-c**. Compound **12** was synthesized from intermediate **6** through a Heck reaction with isobutyl but-3-enoate followed by hydrolysis with sodium hydroxide (Scheme **2**). The mini-PEG analogues **15a-c** were also prepared from the intermediate **9** (Scheme **3**). Coupling of acid **9** with amine-PEG-azide, followed by Pd/C-catalyzed reduction of the azides with hydrogen led to the monoamine derivatives **14a-c**. After a second coupling reaction with acid **9** using HATU as a coupling reagent, the monoamine derivatives **14a-c** were converted into the corresponding dimers **15a-c.**

Scheme 1. Synthesis of **10a-10f**[a]

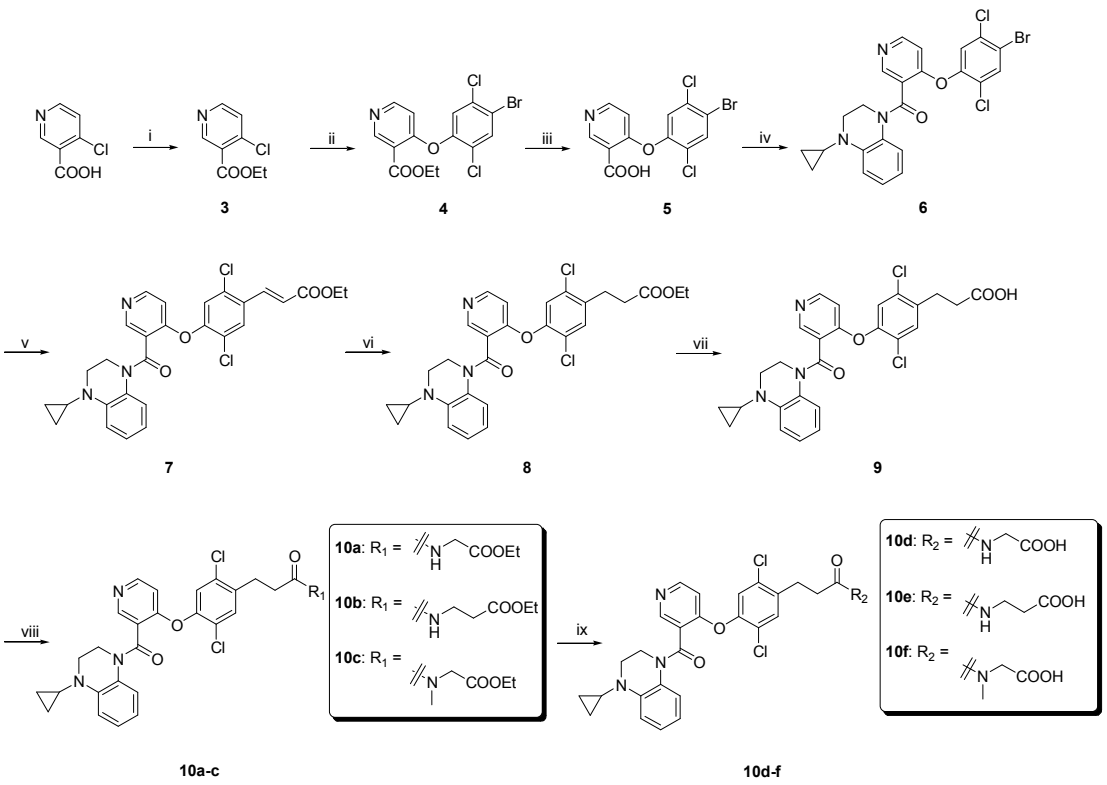

[a]Reagents and conditions: (i) (a) $SOCl_2$, reflux; (b) EtOH, Et_3N, rt, 81%; (ii) 4-bromo-2,5-dichlorophenol, K_2CO_3, DMF, 100 °C, 65%; (iii) NaOH, 1,4-dioxane, H_2O, rt; (iv) (a) $(COCl)_2$, DMF, DCM, reflux; (b) 1-cyclopropyl-1,2,3,4-tetrahydroquinoxaline, Et_3N, DCM rt, 62% for steps iii and iv; (v) ethyl acrylate, $Pd(OAc)_2$, P(*o*-MePh)$_3$, CH_3CN, Microwave, 140 ^oC, 76%; (vi) $NaBH_4$, CuCl, THF, MeOH, 0-5 ^oC, 82%; (vii) NaOH, 1,4-dioxane, H_2O, rt, 92%; (viii) HATU, amino acid ester, Et_3N, DCM, rt, 73-81%; (ix) NaOH, 1,4-dioxane, H_2O, rt, 85-90%.

Scheme 2. Synthesis of **12**[a]

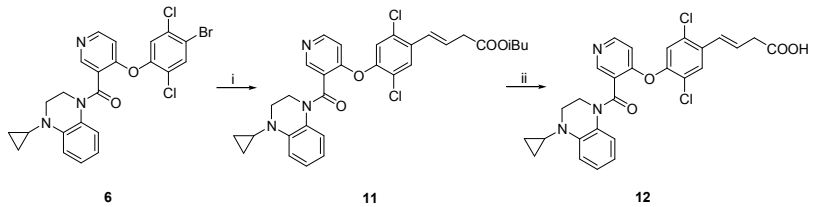

[a]Reagents and conditions: (i) isobutyl but-3-enoate, $Pd(OAc)_2$, P(*o*-MePh)$_3$, CH_3CN, Microwave, 140 ^oC, 39%; (ii) NaOH, 1,4-dioxane, H_2O, rt, 86%.

Scheme 3. Synthesis of PEG Derivatives[a]

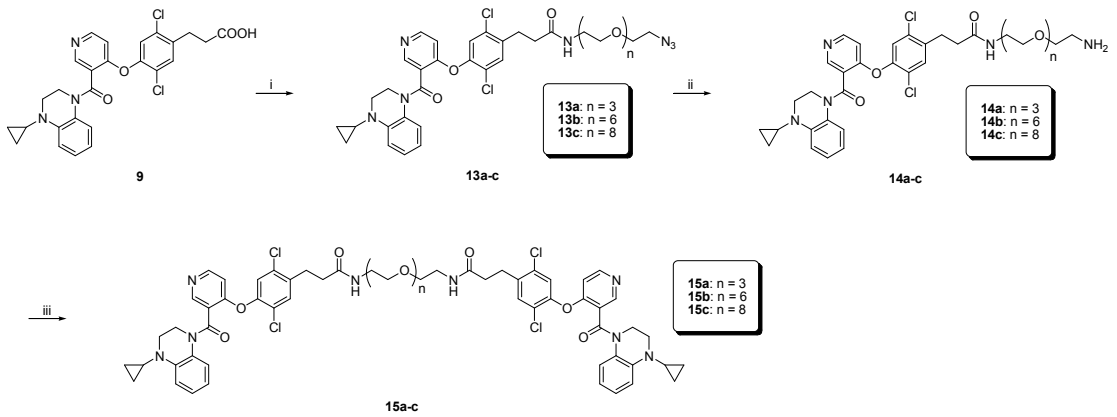

[a]Reagents and conditions: (i) HATU, Et_3N, NH_2-PEG-N_3, DCM, rt, 71%-78%; (ii) H_2, Pd/C, rt; (iii) **9**, HATU, Et_3N, DCM, rt, 49%-63% for steps ii and iii.

RESULTS AND DISCUSSION

A series of carboxylic acid functional groups was incorporated at the 4-position of the phenoxy moiety (Table **1**), and our goal was that these carboxylic acids could couple with amino acids or mini-PEG chains. *In vitro* TGR5 assays demonstrated acceptable TGR5 potency for the propanoic acid analogue **9** and marginal activity for the butenoic acid analogue **12**. The propanoic acid analogue **9** was therefore selected for further derivatization.

Table 1. *In Vitro* Activity of Compounds **8**, **9** and **12**.[a]

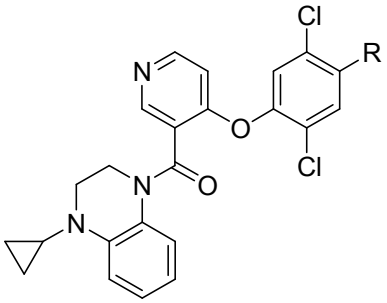

Compd	R	hTGR5 EC_{50} (nM)	mTGR5 EC_{50} (nM)
8	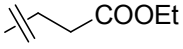	3.8±1.0	11±2.0
9	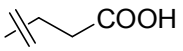	35±1.3	71±7.9

12	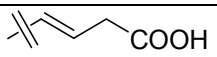	378±86	405±72

[a]EC_{50} values given are expressed as the mean ± SD of three independent experiments.

Several amino acids were linked to **9** through an amide bond, and all of these derivatives exhibited low nanomolar TGR5 activity and greater potency than the parent compound **9** (Table **2**). In contrast to previously reported TGR5 agonists in which the mTGR5 potency was usually much weaker than hTGR5 potency, these derivatives expressed mTGR5 potency comparable to hTGR5 potency. Of note, compounds **10d**, **10e**, and **10f** exhibited greater potency toward mTGR5 than hTGR5. Introduction of amino acids greatly increased the PSA value, with most of the derivatives possessing PSA values of greater than 100 $Å^2$. A maximum PSA value of 112 $Å^2$ was observed for compound **10d**, and this compound was chosen for further *in vivo* pharmacokinetic studies.

Table 2. *In Vitro* Activity of Compounds **10a**−**f**.[a]

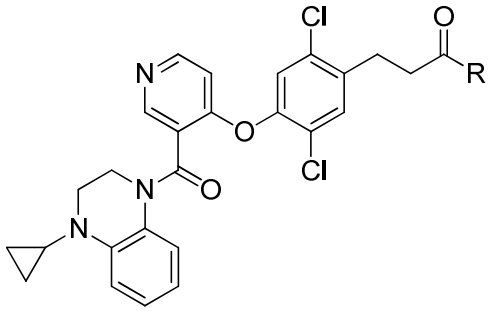

Compd	R	hTGR5 EC_{50} (nM)	mTGR5 EC_{50} (nM)	PSA ($Å^2$)[b]
10a	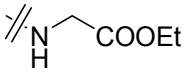	5.3±1.9	5.7±1.4	101
10b	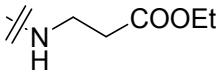	12±3.9	17±2.6	101
10c	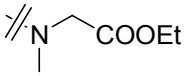	5.0±2.2	7.8±2.4	92

10d	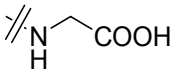	9.6±1.1	8.0±3.1	112
10e	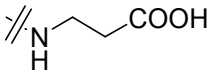	8.0±2.4	3.3±0.90	112
10f	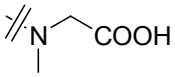	15±4.8	5.8±2.6	103

[a]EC_{50} values given are expressed as the mean ± SD of three independent experiments. [b]PSA values were calculated using MarvinSketch 5.2.5.1.

Subsequent pharmacokinetic testing in rats indicated that **10d** exhibited a low but could not be neglected plasma exposure, with a C_{max} of 13.5 ng/mL after a 5 mg/kg oral dose (Table **3**). In order to evaluate the *in vivo* glucose-lowering activity of **10d**, an oral glucose tolerance test (OGTT) was carried out using ICR mice. Following oral administration of **10d** (50 mg/kg), the area under the glucose levels versus time curve $(AUC)_{0\text{-}120min}$ was decreased by 33% compared to the control group (Figure **2A** and **2B**). A further *in vivo* study in ICR mice revealed an 82% increase in GLP-1 concentration following administration of **10d** compared to the control group (Figure **2C**). Combined treatment with **10d** and Linagliptin (BI-1356, (R)-8-(3-amino-piperidin-1-yl)-7-but-2-ynyl-3-methyl-1-(4-methyl-quinazolin-2-ylmethyl)-3,7-dihydro-purine-2,6-dione), a DPP-4 inhibitor developed by Boehringer Ingelheim,[36] increased secretion of GLP-1 by 64% compared to Linagliptin alone (Figure **2D**). Unfortunately, gallbladder area increased approximately 225% relative to the control group (Figure **3**).

Table 3. PK properties of **10d**, **15c**, and the metabolite **9** following administration of **10d** or **15c** to rats.[a]

Compd	T_{max} (h)	C_{max} (ng/mL)	$AUC_{0\text{-}t}$ (ng*h/mL)	$AUC_{0\text{-}\infty}$ (ng*h/mL)	MRT (h)	$T_{1/2}$ (h)
10d	0.44	13.5	23.9	39.7	2.37	1.56
9[b]	3.50	15.5	84.9	241	5.47	1.77
15c	-[d]	-	-	-	-	-
9[c]	-	-	-	-	-	-

[a]n = 4 rats/group; male SD rats (BK, Shanghai, China); p.o., 5 mg/kg for **10d**, 20 mg/kg for **15c**; formulated in 0.25% CMCNa; PK parameters were calculated by WinNonlin 5.3. [b]Data for metabolite **9** following administration of **10d**. [c]Data for metabolite **9** following administration of **15c**. [d]'-' indicates 'no desired compound was detected'.

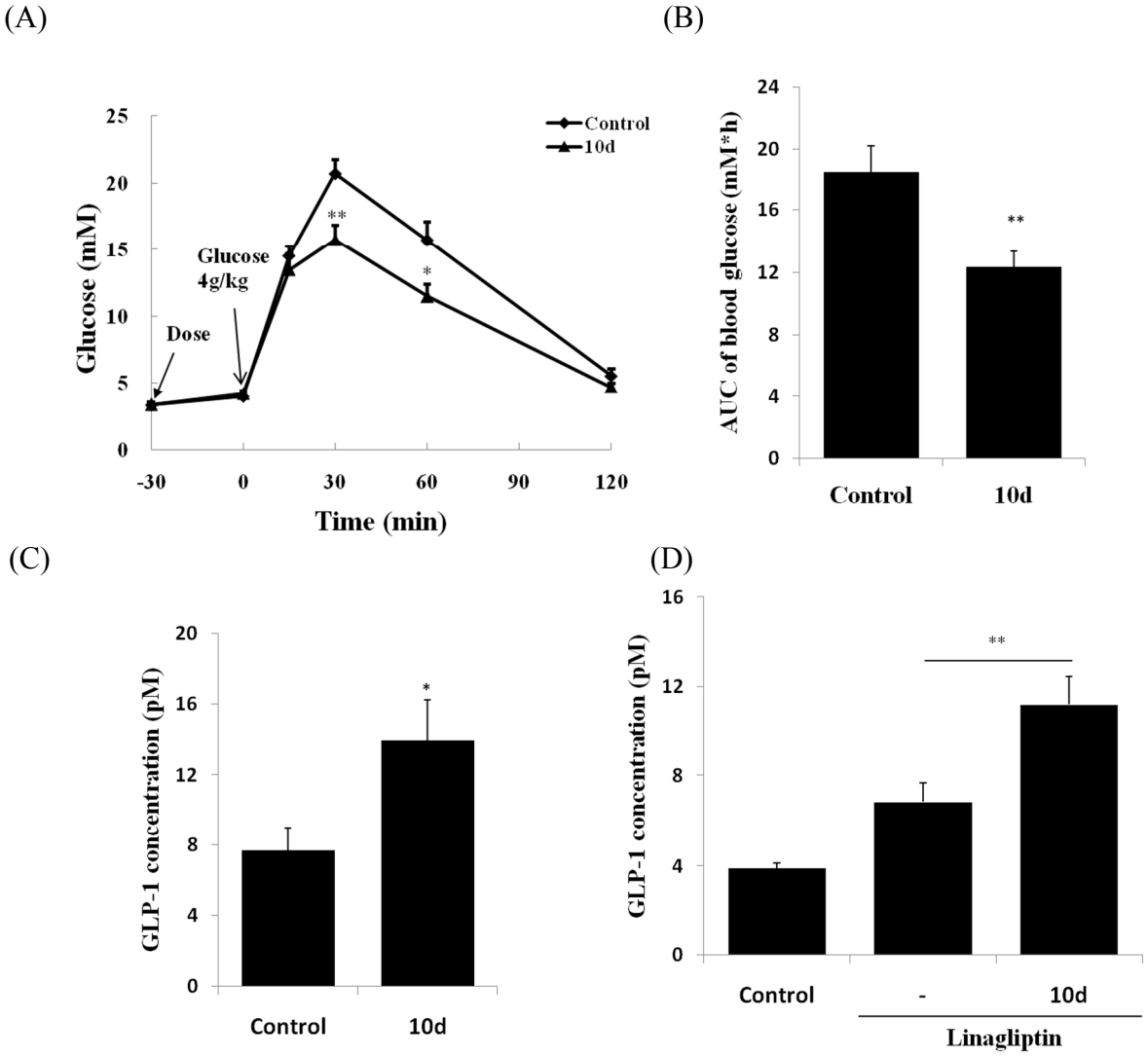

Figure 2. OGTT and GLP-1 secretion study of **10d** (50 mg/kg) in ICR mice: (A) blood glucose concentration after administration of **10d**; (B) blood glucose $AUC_{0-120\ min}$ after administration of **10d**. For (A) and (B): Compound **10d** or 0.25% CMC (control) were administered orally to ICR mice (n = 8 animals/group) at 0.5 h prior to oral glucose load (4 g/kg). Blood glucose levels were measured before and after glucose load. (C) GLP-1 secretion study of **10d**. Compound **10d** or

0.25% CMC (control) were orally administered to ICR mice (n = 10 animals/group) 0.5 h prior to oral glucose load (4 g/kg). Blood samples were collected 5 min after glucose challenge. (D) GLP-1 secretion study of **10d** combined with Linagliptin. Linagliptin was orally administered to ICR mice (n = 8-10 animals/group) 1 hour prior to compound **10d** or 0.25% CMC (control) dosing. 4 Hours after compounds or control administration, blood samples were collected. All the blood samples were placed in Eppendorf tubes containing DPP-4 inhibitor with final concentrations of 1% blood samples and 25 mg/mL EDTA to measure serum active GLP-1[7–36 amide] levels. ∗, $P < 0.05$; ∗∗, $P < 0.01$ versus control. Error bar indicates SEM.

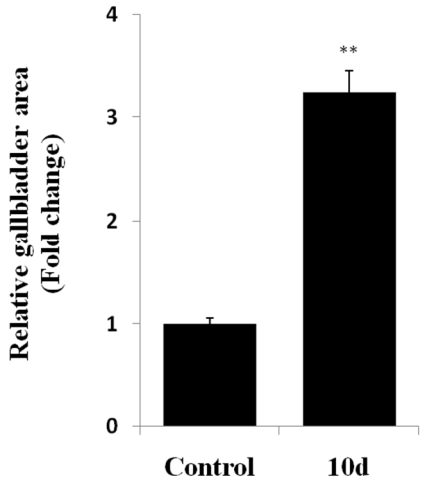

Figure 3. Relative area of gallbladder after **10d** (50 mg/kg) or 0.25% CMC (vehicle) was orally administered to ICR mice (n = 8 animals/group). Following the OGTT experiment, the fasting mice were refed for 2 h. The gallbladders were removed, and the area was measured using a vernier caliper. The area of the gallbladder was measured by the length of the gallbladder multiplied by the width of the gallbladder. ∗∗, $P < 0.01$ versus control. Error bar indicates SEM.

(A) (B)

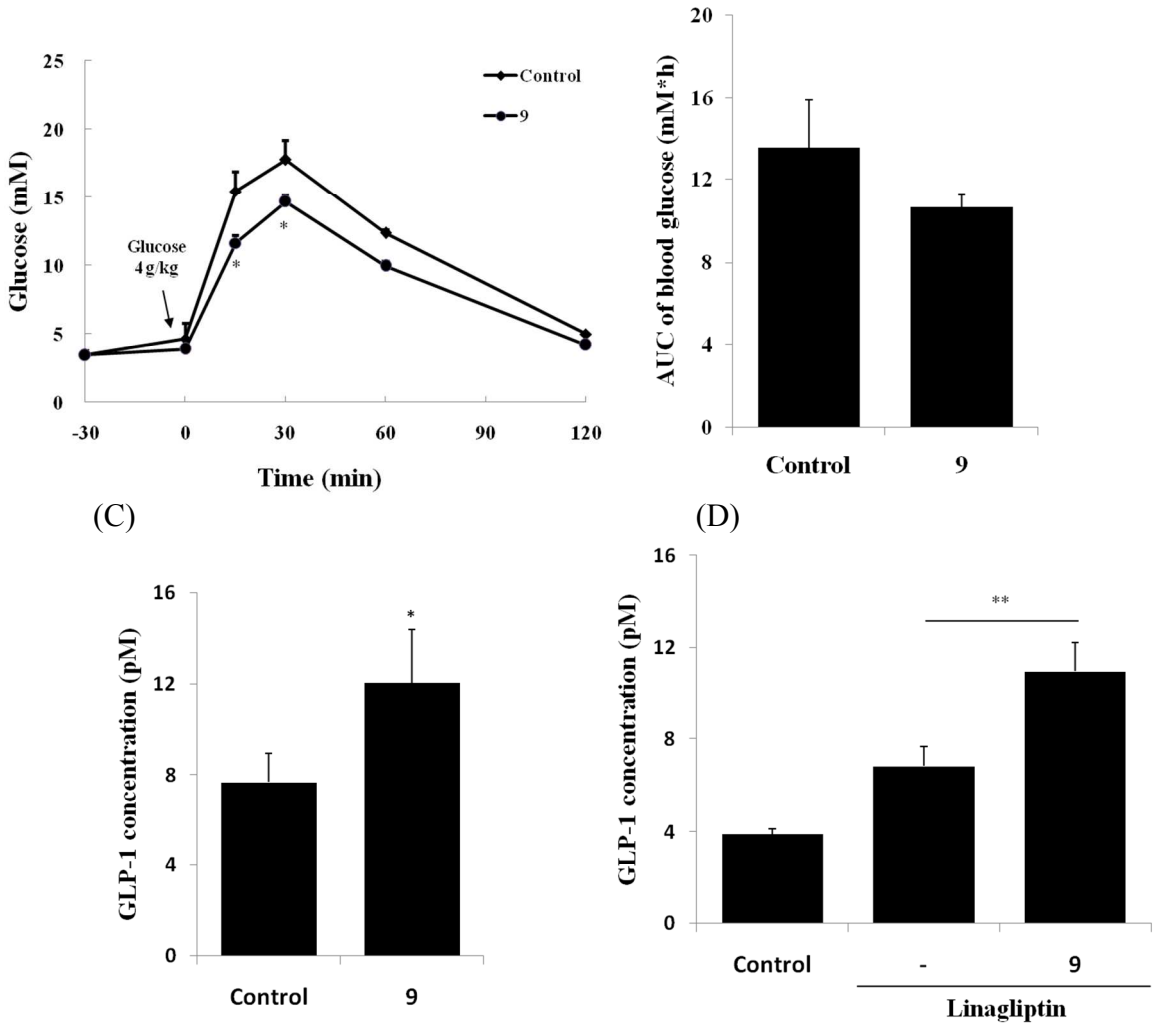

Figure 4. OGTT and GLP-1 secretion study following administration of compound **9** (50 mg/kg) in ICR mice: (A) blood glucose concentration; (B) blood glucose $AUC_{0-120\ min}$. (C) GLP-1 secretion. (D) GLP-1 secretion study after administration of **9** combined with Linagliptin. ∗, $P < 0.05$; ∗∗, $P < 0.01$ versus control. Error bar indicates SEM.

We suspected that the severe side effect occurring after administration of **10d** was due to the combined effects of **10d** and its pharmacologically active metabolites. Pharmacokinetic studies (0-24 h) revealed that the main metabolite (compound **9**, mTGR5 EC_{50} = 71 nM) was formed by hydrolysis of the amide bond of the parent compound. The metabolite **9** was observed in the

plasma with a similar C_{max} (15.5 ng/mL), but a higher AUC compared to the parent drug (Table **3**, Figure **S1**), and was demonstrated to be an active metabolite capable of activating TGR5 *in vivo* and lowering the blood glucose levels (Figure **4A** and **4B**). After oral administration of compound **9** (50 mg/kg), GLP-1 levels increased by 57% compared to the control group (Figure **4C**). When used in combination with Linagliptin, compound **9** also increased secretion of GLP-1 by 55% compared to Linagliptin alone (Figure **4D**). The combined activation of TGR5 by the parent compound and active metabolite may lower the glucose concentrations and cause the increase in gallbladder area.

Table 4. *In Vitro* Activity of Compounds **15a**−**c**.[a]

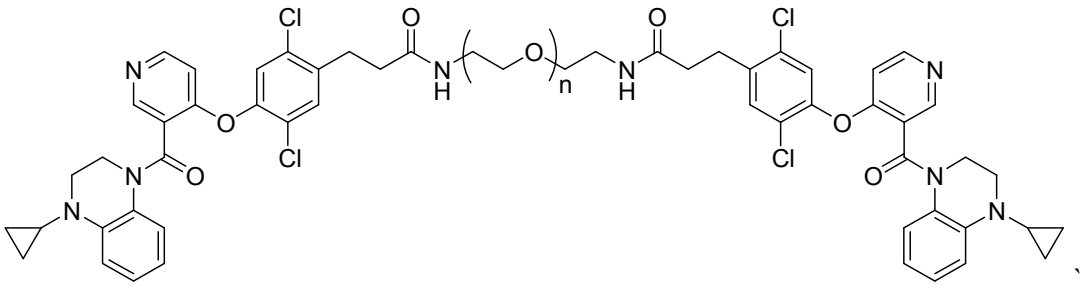

Compd	n	MW	PSA (Å^2)[b]	hTGR5 EC_{50} (nM)	mTGR5 EC_{50} (nM)
15a	3	1181	177	30±13	14±1.0
15b	6	1313	205	20±8.2	13±1.4
15c	8	1401	223	25±1.7	12±2.9

[a]EC_{50} values are expressed as the mean ± SD of three independent experiments. [b]PSA values were calculated using MarvinSketch 5.2.5.1.

Table 5. Apparent permeability in Caco-2 cells.[a]

Compd	A to B		B to A		Efflux Ratio
	Papp (10^{-6} cm/s)	Recovery (%)	Papp (10^{-6} cm/s)	Recovery (%)	
2	6.75±1.61	46.8±1.7	5.58±0.58	69.4±0.7	0.8

15c	0.04±0.01$^{\#\#}$	99.5±4.2	2.24±0.19$^{**, \#\#}$	91.2±1.5	61
Digoxin	0.1±0.03	100.8±0.5	15.8±4.5	95.8±0.3	153

[a]'A to B' indicates the experiment from apical to basolateral, 'B to A' indicates the experiment from basolateral to apical. **, P <0.01 versus Papp (A to B) of **15c**; ##, P <0.01 versus Papp of **2**.

Considering that **10d** may still be absorbed to some extent, compounds with a much higher PSA and lower permeability may be necessary to avoid activation of TGR5 receptors in the gallbladder. A series of dimeric TGR5 agonists **15a-c** containing a mini-PEG linker was designed and synthesized (Table **4**). The molecular weights of these analogues were greater than 1000, and we expected them to be poorly absorbed from the intestine based on Lipinski's rule.[33] The PSA values of the PEG_3 derivative **15a**, the PEG_6 derivative **15b**, and the PEG_8 derivative **15c** were 177, 205, and 223 $Å^2$, respectively. Although introduction of PEG chains to dimeric TGR5 represented a substantial departure from the original structure, the potency did not decrease. The mTGR5 EC_{50} values for **15a-c** were 14, 13, and 12 nM, and the hTGR5 EC_{50} for **15a-c** were 30, 20, and 25 nM. The length of the PEG linker did not have a large effect on the potency. The PEG_8 derivative **15c** was selected for further study due to its higher molecular weight and greater PSA. In Caco-2 permeability assays, compound **15c** exhibited a much lower permeability than the small-molecule TGR5 agonist **2** (Table **5**).

To determine the systemic exposure of **15c**, a pharmacokinetic study was carried out (Table **3**). Following administration of an oral dose of **15c** (20 mg/kg) to rats, blood samples were obtained and analyzed (15 min - 24 h). There were no detectable (LLOQ = 3 ng/mL) levels of the parent compound **15c**, the potential metabolite **9**, or any other major metabolites in the systemic circulation.

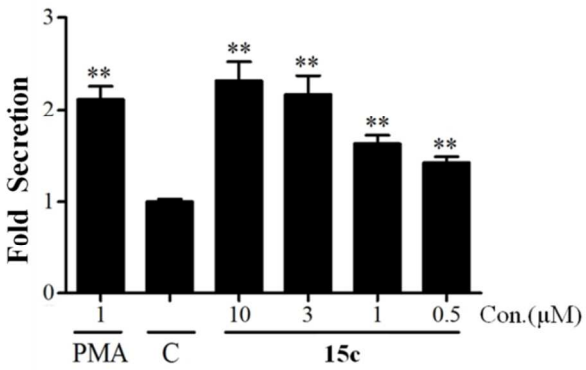

Figure 5. GLP-1 secretion by NCI-H716 cells in response to a 2-h treatment with PMA (1 μM, positive control), vehicle (control), or **15c** (10 , 3, 1, and 0.5 μM). Data shown are expressed as the mean ± SEM of three independent experiments. **, $P < 0.01$ versus control.

Next, we examined the *in vivo* glucose-lowering activity of **15c** using an OGTT in ICR mice. Considering the high molecular weight, the oral dose of **15c** was increased to 150 mg/kg (0.11 mmol/kg). As shown in Figure **6A** and **6B**, the $(AUC)_{0\text{-}120\ min}$ for glucose levels versus time decreased 30% compared to the control group. Following a single dose, **15c** significantly lowered glycemia at time points of 15 and 30 min. Compound **15c** exhibited a comparable glucose-lowering effect with absorbed TGR5 agonist **2**.

We also evaluated the GLP-1 secretion effect of **15c**. Treatment of NCI-H716 cells with **15c** at 0.5, 1, 3, and 10 μM concentrations, GLP-1 secretion increased in a dose-dependent manner (Figure **5**). A further *in vivo* study in ICR mice was also carried out. After a single oral administration, the plasma active GLP-1 level was increased by 97% compared to the control group (Figure **6C**). Besides, compound **15c** also increased basal secretion of GLP-1. The combination of **15c** and Linagliptin enhanced GLP-1 secretion by 61% compared to Linagliptin alone (Figure **6D**).

Following oral administration of **15c** (150 mg/kg) to ICR mice, the gallbladder area increased

approximately 44% compared with the control group, which was not a significant difference (Figure **7**). This is in sharp contrast to compound **2**, which increased gallbladder area several-fold after an oral dose of 50 mg/kg.

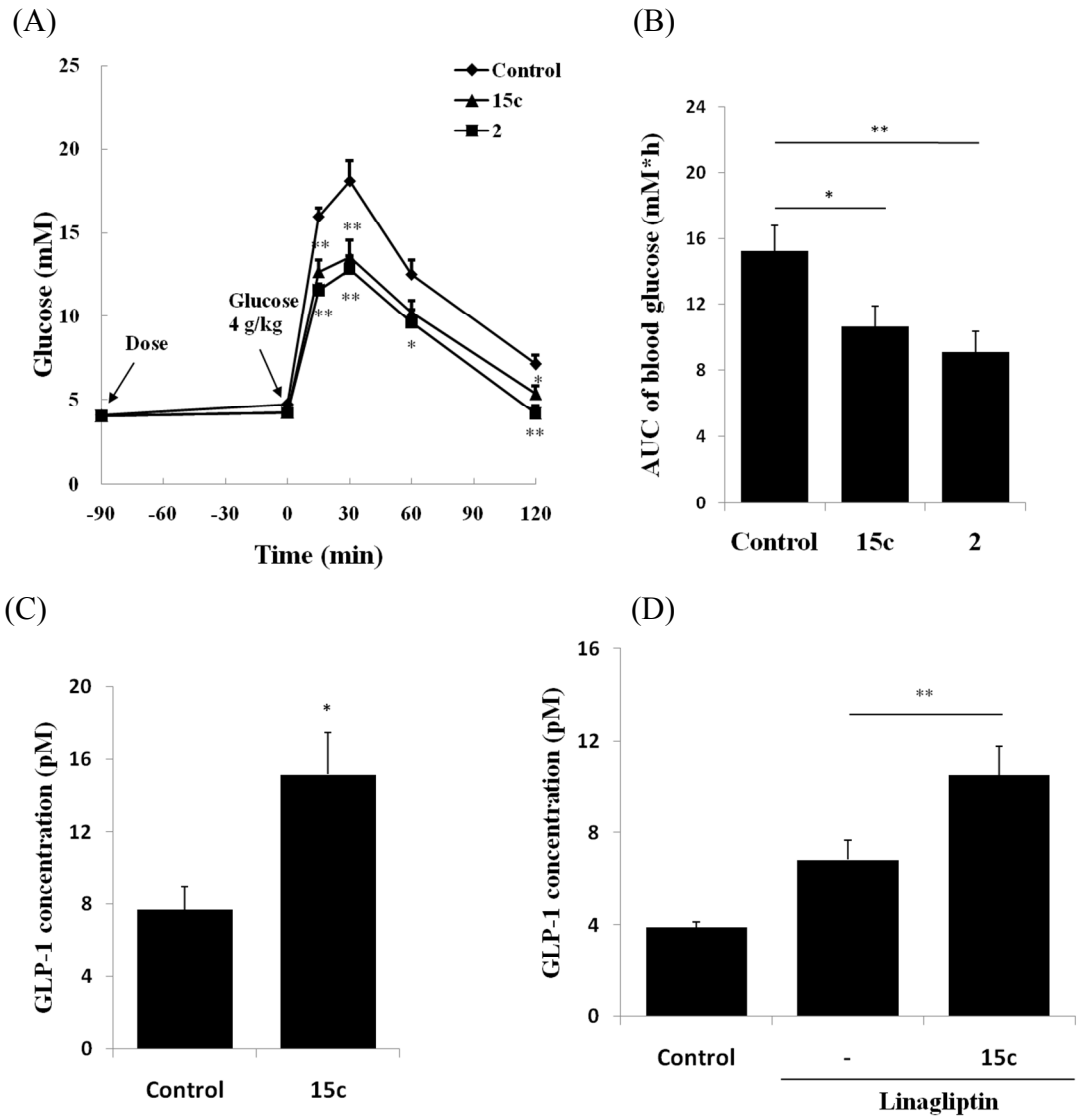

Figure 6. OGTT of **15c** (150 mg/kg) and **2** (50 mg/kg) and GLP-1 secretion study of **15c** (150 mg/kg) in ICR mice: (A) blood glucose of **15c** and **2**; (B) blood glucose $AUC_{0-120\ min}$ of **15c** and **2**. (C) GLP-1 secretion study of **15c**. Compound **15c** or 0.25% CMC (control) was orally administered to ICR mice (n = 10 animals/group) 1.5 h prior to the oral glucose load (4 g/kg). (D)

GLP-1 secretion study of **15c** combined with Linagliptin. ∗, P < 0.05; ∗∗, P <0.01 versus control. Error bar indicates SEM.

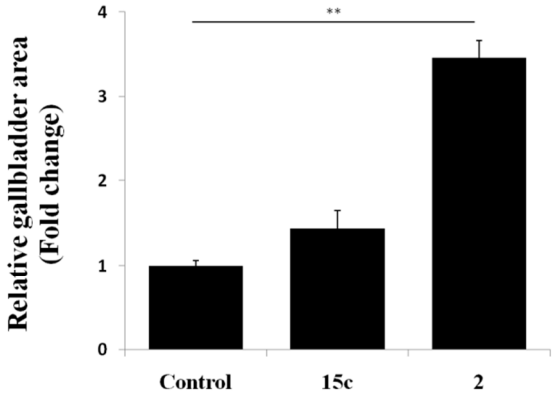

Figure 7. Relative area of gallbladder after compound or 0.25% CMC (control) was orally administered to ICR mice (n = 8 mice/group). Compound dose: 150 mg for **15c**, 50 mg/kg for **2**. The fasting mice were refed for 2 h after the OGTT experiment, then, the gallbladders were removed, and the area was measured using a vernier caliper. The relative area of the gallbladder was calculated from the length multiplied by the width of the gallbladder. ∗∗, P < 0.01 versus control. Error bar indicates SEM. Data are representative of three independent experiments.

We further analyzed the drug levels of **15c** in the gallbladder. As depicted in Figure **8**, four hours after oral administration of **15c** (150 mg/kg) there was no parent drug present in the gallbladder tissue (< 0.3 ng) and the metabolite **9** was only present at a low concentration. The bile concentrations of **15c** and **9** were far lower than the concentration of **2** after oral administration of 50 mg/kg.

In another PK experiment, we treated ICR mice with the same dosing as used in the OGTT experiment, 150 mg/kg p.o. of **15c**, and measured the drug levels in plasma, bile, and gallbladder tissue at time 2, 2.5, and 3.5 h after administration. As shown in Table **6**, only nanomolar levels

of **15c** were detected in the plasma and the bile, below the EC_{50} of **15c** (mTGR5 EC_{50} = 12 nM). The low concentrations of **15c** in plasma, bile, and gallbladder tissue demonstrated that **15c** was a low-absorbed TGR5 agonist. The glucose lowering effect was due to its specific activation of TGR5 in the intestine, and this maybe the reason for the decreased gallbladder side effects.

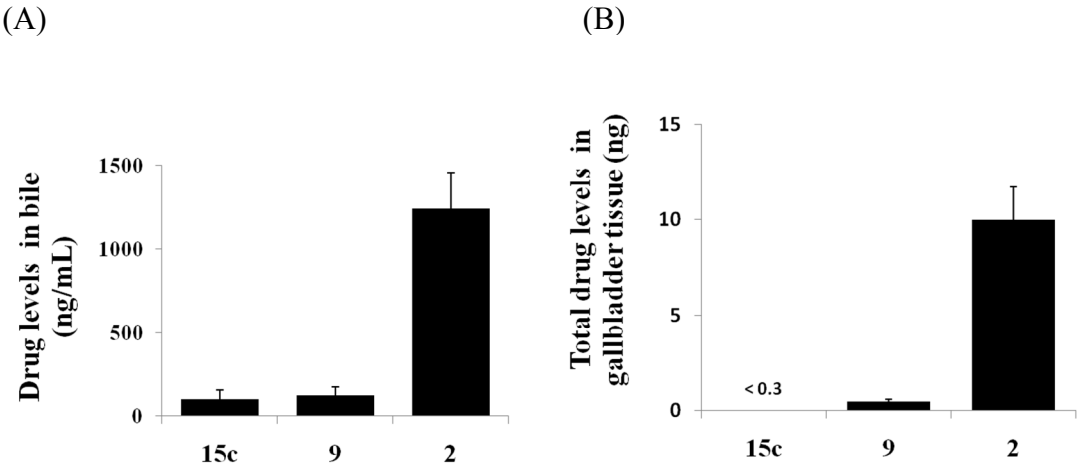

Figure 8. Drug levels of compound **15c** (150 mg/kg), **9** (metabolite after orally dosed **15c**) and **2** (50 mg/kg) in gallbladder 4 h after oral administration to ICR mice. (A) Drug levels in bile; (B) Total drug levels in gallbladder tissue. n = 4−7 mice/group. Error bar indicates SEM.

Table 6. Drug levels of compound **15c** in plasma, bile, and gallbladder tissue after oral administration to ICR mice.[a]

Time (h)	Sample location		
	Plasma (ng/mL)	Bile (ng/mL)	Gallbladder tissue (ng/g)
2	6.22 (4.4 nM)	5.07 (3.6 nM)	-[b]
2.5	9.65 (6.9 nM)	4.93 (3.5 nM)	-
3.5	4.03 (2.9 nM)	5.33 (3.8 nM)	-

[a]Drug levels of compound **15c** in plasma, bile and gallbladder tissue after oral administration to ICR mice (150 mg/kg). (A) Drug levels in bile; (B) Total drug levels in gallbladder tissue. n = 3

mice/group. [b]'-' indicates 'no desired compound was detected'.

The appearance of **15c** in the gallbladder indicated that there was still some parent compound absorbed from the intestine, and an even longer PEG linker may be beneficial to further decrease the absorption. Considering the active metabolite **9** originates from hydrolysis of the amide bond to the PEG, it may be beneficial to introduce bulky groups to the amide to increase steric hindrance and improve resistance to hydrolysis, or to replace the amide bond with an inherently more resistant ether or amine linkage. The effectiveness of the mini-PEG linkage suggested that there may be a large pocket available on the TGR5 receptor, and that other hydrophilic groups, such as quaternary ammonium salts or polyhydric derivatives could also be incorporated into the 4-phenoxynicotinamide scaffold to prepare some non-absorbed TGR5 agonists while maintaining the potency.

Conclusion

In summary, introduction of polar, hydrophilic groups to the 4-phenoxynicotinamide derivative **2** as well as dimerizing the core structure using a PEG-linker led to a series of low-absorbed TGR5 agonists. Due to the low intestinal absorption, compound **15c**, which displays *in vivo* glucose lowering effects comparable to the absorbed TGR5 agonist **2**, reduced the gallbladder side effect a lot compared to **2**. As the first low-absorbed TGR5 agonist to be reported, **15c** represents a useful prototype compound in the development of other non-absorbed TGR5 agonists for diabetes treatment.

EXPERIMENTAL SECTION

In Vitro TGR5 Assay.

hTGR5/CRE/HEK293 or mTGR5/CRE/HEK293 stable cell line was obtained by transfection

of HEK293 cells with human or mouse TGR5 expression plasmid (hTGR5-pcDNA3.1 or mTGR5-pcDNA3.1) and CRE-driven luciferase reporter plasmid (pGL4.29, Promega, Madison, WI), and employed to assess the activity of test compounds by reporter gene assay. Briefly, cells were seeded into 96-well plates and incubated overnight in DMEM supplemented with 10% FBS in 5% CO_2 at 37 °C. Then, cells were incubated with fresh medium containing different concentrations of test compounds or 20 μM compound **1** as a positive control for 5.5 hours. Luciferase activity in cell lysate was determined using the Steady-Glo® Luciferase Assay System (Promega, Madison, WI) according to the manufacturer's instructions. Assays were performed for at least 3 times.

***In Vitro* GLP-1 Assay.**

NCI-H716 cells were maintained in suspension culture as described by American Type Culture Collection. Forty-eight hours before the assay, cells were planted into 24-well plates coated with Matrigel (BD Biosciences, Oxford, UK). On the assay day, cells were washed with KREBS and then incubated with test reagents diluted in KREBS (with 0.2% BSA and 1% DPP-4 inhibitor) for 2 h at 37 °C. After incubation, buffer was collected and centrifuged to remove floating cells. Concentrations of GLP-1 in the buffer were assayed using active GLP-1 ELISA-kit from Millipore.[37,38] Results were mean of three independent assays in duplicate.

Animals.

Male ICR mice (7-8 weeks) were purchased from the Shanghai SLAC Laboratory Animal Co. Ltd (Shanghai, China). The animals were maintained under a 12-h light-dark cycle with free access to water and food. Animal experiments were approved by the Animal Care and Use Committee, Shanghai Institute of Materia Medica, Chinese Academy of Sciences.

GLP-1 Secretion in ICR Mice.

Glucose stimulated GLP-1 secretion: compounds **9** (50 mg/kg), **10d** (50 mg/kg) and **15c** (150 mg/kg) were orally administered to overnight fasting male ICR mice (n = 9-10 animals/group, 7-8 weeks). Compound **15c** was given 1.5 hours prior to glucose challenge. Compound **9** and **10d** were given 0.5 hour prior to the glucose challenge. Then all the mice were challenged with 4 g/kg glucose, and blood samples were collected at 5 mins after glucose loading.

Basal GLP-1 secretion: male ICR mice were fasted for 6 hours. Linagliptin (3 mg/kg) was orally given to all the mice except vehicle control group. 1 Hour later, compound **9** (50 mg/kg), **10d** (50 mg/kg) and **15c** (150 mg/kg) were orally given to the mice. Blood samples were collected 4 hours after compounds dosing.

All the blood samples were placed in Eppendorf tubes containing the DPP-4 inhibitor (Millipore, DPP-4-010) with a final concentration of 1% blood samples and 25 mg/mL EDTA to measure serum active GLP-1[7-36 amide] levels. All the compounds were evaluated in one examination, so Figure **2C**, **4C**, **6C** share the same control, and Figure **2D**, **4D**, **6D** share the same control

Oral Glucose Tolerance Test (OGTT) and Gallbladder Area Measurement in ICR Mice.

To examine the acute effect of compounds on blood glucose after an oral glucose challenge, test compounds or vehicle (0.25% CMC) were orally administered to overnight fasting male ICR mice (n = 8 mice/group, 7-8 weeks) 0.5 (**10d** and **9**) or 1.5 (**15c**) h prior to the oral glucose load (4 g/kg). Blood glucose levels were measured via blood drops obtained by clipping the tail of the mice using an ACCU-CHEK Advantage II Glucose Monitor (Roche, Indianapolis, IN) before compound dosing and 0, 15, 30, 60 and 120 min after the glucose load. The area under the concentration–time curve from 0 to 120 min ($AUC_{0\text{-}120min,\ Glu}$) of blood glucose after the glucose load was calculated by the trapezoidal rule (using the 0 time glucose level for each animal as that

animal's baseline). After the OGTT experiment, the fasting mice were re-fed for 2 h. Then, gallbladders were removed, and the area was measured using vernier caliper.

PK experiment in SD rats.

Male SD rats (200-220 g) were obtained from Shanghai SLAC Laboratory Animal Co. Ltd (Shanghai, China). Compound **10d** (5 mg/kg), or **15c** (20 mg/kg) was orally administered to 12-fasting SD rats (n = 4). Blood samples were collected at different time points. After centrifugation (11000 rpm, 5 min) of the blood, plasma was isolated. 25 μL of the sample was mixed with 12.5 μL of methanol, 12.5 μL of H_2O and 25 μL of phenacetin solution (1000 ng/mL). After centrifugation at 11000 rpm for 5 mins, the supernatant was analyzed by LC-MS/MS. We tested the drug levels of different time points from 0.25 h to 24 h, and we chose one of the time points with the highest drug concentration as the C_{max} and T_{max} (Figure **S1**). The other parameters were calculated based on the drug-time curve by WinNonlin 5.3.

Caco-2 permeability determination

Caco-2 cells were obtained from the ATCC (HTB-37) and maintained in DMEM containing 10% FBS, 1% glutamine, 1% nonessential amino acids, 100 mg/mL penicillin and streptomycin. Caco-2 cells were cultured at 37 ^{o}C in a 5% CO_2 and 90% relative humidity environment. Cells were used between passages 30 and 40. After 21 days of culture, the integrity of the cell monolayer was verified by measuring the transepithelial electrical resistance (TEER). Drug transport from the apical side to the basolateral side (A-B) and from the basolateral side to the apical side was measured under the same condition. To verify our model is proper for both compounds with low and high permeabilities, propranolol (high permeability) and atenolol (poor permeability) were used as the external hypertonic and hypotonic control, respectively. For the experiment, the Papp values of propranolol are 19.2×10^{-6} cm/s (A to B) and 12.9×10^{-6} cm/s (B

to A). The Papp values of propranolol are 0.1×10^{-6} cm/s (A to B) and 0.6×10^{-6} cm/s (B to A). The data indicates that this model works well for both high and low permeable compounds. Digoxin was used as the positive control for Pgp-mediated drug efflux. The concentrations for the tested compounds are 20 μM. In brief, the method was as follows. After washing the monolayer with HBSS three times, the compounds were diluted and added to the appropriate well (pH 6.8 for apical side and pH 7.4 for basolateral side). The plate was incubated at 37 ^{o}C for 95 min. Samples were collected from the donor side at 5 and 95 min, and from the receiver side at 35 and 95 min post-incubation. The concentration of samples was measured by LC-MS/MS. The Papp was calculated from the following equation: $Papp = (V_A/(SA \times T)) \times ([drug]_{acceptor}/[drug]_{initial\ donor})$. Where V_A is the volume of the acceptor well, SA is the surface area of the membrane, T is the total transport time, $[drug]_{acceptor}$ is the drug level at the acceptor side, and $[drug]_{initial\ donor}$ is the drug level at the donor side at T = 0.

Drug Levels Test in Bile, and Gallbladder Tissue after Oral Administration to ICR Mice.

Compound **15c** (150 mg/kg) or **2** (50 mg/kg) was administered orally to male ICR mice (7-8 weeks). Bile and gallbladder tissue were collected at different time points post-dose for drug levels test. Briefly, gallbladder was homogenized after adding 100 μL of methanol. A 15 μL aliquot of bile samples were diluted with 100 μL of methanol and then mixed. Bile and tissue homogenate were stored at −20 °C. These samples were protein precipitated with acetonitrile using clopidogrel as the internal standard, and the supernatant was injected onto LCMS/MS system for the quantification. Chromatographic separation was performed on a luna C_{18} column (50 mm × 2.0 mm ID, 5 μm, Phenomenex, Torrance, CA, USA) using 5 mM ammonium acetate and acetonitrile (1: 1, v/v) containing 0.02% formic acid as the mobile phase, which was delivered at a flow rate of 0.8 mL/min. The MS detection was carried out in multiple reactions

monitoring mode using a positive electrospray ionization interface. The calibration curve of compound was established from 3.0 to 3000 ng/mL for bile, and from 3.0 to 3000 ng/g for gallbladder tissue. To confirm accuracy, quality control samples were analyzed in duplicate at three different concentrations. The bioanalytical run meet the acceptance criteria which require that at least 3/4 of the calibration standards were within 15% of theoretical and that greater than 2/3 of all quality control samples were within 15% of theoretical. All the equipments and parameters for the drug levels test and PK experiment were list in supporting information.

Statistical Analysis.

All data were expressed as the Mean ± SEM. For the experiment including multiple time points, one-way ANOVA statistical analysis was used, otherwise, unpaired Student's *t* test was used.

Synthetic Materials and Methods.

All reagents were purchased from commercial suppliers and used without further purification. ^{1}H NMR and ^{13}C NMR spectra were recorded on a Brucker AC300 or a Brucker AC400 NMR spectrometer using tetramethylsilane as an internal reference. ESI-MS spectra were obtained on a Krats MS 80 mass spectrometer. The purity of tested compounds was determined by HPLC (Agilent LC1200, Agilent ChemStation, Agilent Eclipse XDB-C18, 5 μM, 4.6×150 mm, UV 254 nM, 30 ^{o}C, Flow Rate = 1.0 mL/min). All the assayed compounds possess > 95% purity. Column chromatography was performed on silica gel (200-300 mesh).

Ethyl 4-Chloronicotinate (3). 4-Chloronicotinic acid (3.0 g, 19.1 mmol) was dissolved in thionyl chloride (30 mL), and the solution was refluxed for 1.5 h. Then the solvent was removed under reduced pressure. The residue was dissolved in toluene (5 mL) and concentrated to dryness. Then ethanol (30 mL) and triethylamine (5 mL) were added to the residue, and the solution

mixture was stirred at room temperature overnight. After the solvent was evaporated, H_2O (30 mL) was added to the residue, and then extracted with dichloromethane (30 mL × 3). The combined organic phase was washed with saturated solution of sodium bicarbonate (50 mL) and brine (50 mL), and then dried over anhydrous sodium sulfate. The product was purified by flash column chromatography (petroleum ether/ethyl acetate = 8:1) to yield **19** as colorless oil (0.95 g, 81%). LC-MS (ESI+): 186 $(M + H)^+$. ^{1}H NMR (300 MHz, CD_3OD) δ 9.20 (s, 1H), 8.82 (d, J = 6.1 Hz, 1H), 8.08 (d, J = 6.1 Hz, 1H), 4.58 – 4.37 (m, 2H), 1.50 – 1.36 (m, 3H).

Ethyl 4-(2,5-Dichloro-4-bromo-phenoxy)-nicotinate (**4**). To a solution of **3** (1.85 g, 10 mmol) in anhydrous DMF (15 mL), 2,5-dichloro-4-bromophenol (2.4 g, 12 mmol) and potassium carbonate (4.14 g, 30 mmol) were added. After the solution was heated at 100 °C for 3 h, the reaction was cooled to room temperature and poured into H_2O (100 mL). The mixture was extracted with ethyl acetate (100 mL × 3), and the combined organic phase was washed with brine. After dried over anhydrous sodium sulfate, the solvent was evaporated to afford the product. The crude was purified with flash column chromatography (petroleum/ethyl acetate = 4:1) to yield the desired compound in 65% yield. ^{1}H NMR (400 MHz, $CDCl_3$) δ 9.09 (s, 1H), 8.57 (d, J = 5.7 Hz, 1H), 7.26 (s, 1H), 7.22 (d, J = 4.3 Hz, 1H), 6.62 (d, J = 5.8 Hz, 1H), 4.40 (q, J = 7.1 Hz, 2H), 1.37 (t, J = 7.1 Hz, 3H).

[4-(2,5-Dichloro-4-bromophenoxy)-pyridin-3-yl]-(4-cyclopropyl-3,4-dihydro-2*H*-quinoxalin-1-yl)-methanone (6). To a solution of **4** (2.4 g, 6.13 mmol) in 1,4-dioxane (20 mL) and H_2O (20 mL), sodium hydroxide (0.49 g, 6.13 mmol) was added. The reaction was stirred at ambient temperature for 3 h. After the solvent was evaporated, the residue was dissolved in H_2O and pH was adjusted to 3 with 2N hydrochloric acid. The formed precipitated was filtered, washed with cold water and dried under vacuum providing **5**. The obtained compound was

dissolved in dichloromethane (30 mL), and then oxalyl chloride (1.56 mL, 18.4 mmol) was added to the solution. The resulting solution was refluxed for 2 h. After the reaction was completed, the solvent was evaporated and the remaining oxalyl chloride was removed by azeotropic distillation with toluene. After the residue was dissolved in anhydrous dichloromethane, 1-cyclopropyl-1,2,3,4-tetrahydro- quinoxaline (1.07 g, 6.13 mmol) and Et_3N (2.55 mL, 18.39 mmol) were added to this solution. And the reaction was stirred at room temperature for 2 h. After the reaction was completed, the mixture was washed with brine, dried over anhydrous sodium sulfate and purified by flash column chromatography (petroleum/ethyl acetate = 3:1) to provide **6** (1.97 g) in 62% yield for two steps. ^{1}H NMR (300 MHz, $CDCl_3$): δ 8.85 (s, 1H), 8.44 (d, J = 4.2 Hz, 1H), 7.67 (s, 1H), 7.02 (t, J = 5.7 Hz, 1H), 6.94 (d, J = 5.7 Hz, 1H), 6.47 (d, J = 5.7 Hz, 1H), 6.38 (t, J = 5.7 Hz, 1H), 6.30 (d, J = 4.2 Hz, 1H), 5.76 (s, 1H), 4.89 (m, 1H), 3.49 (m, 2H), 3.16 (m, 1H), 2.25 (m, 1H), 0.69 (m, 3H), -0.23 (br, 1H).

(E)-ethyl 3-(2,5-Dichloro-4-((3-(4-cyclopropyl-1,2,3,4-tetrahydroquinoxaline-1-carbonyl)pyridin-4-yl)oxy)phenyl)acrylate (7). To a suspension of **6** (1.04 g, 2.00 mmol) in acetonitrile (15 mL), ethyl acrylate (534 μL, 4.00 mmol), palladium diacetate (89.8 mg, 0.40 mmol), tris(2-methylphenyl)phosphine (243 mg, 0.80 mmol) and triethylamine (1.39 mL, 10.0 mmol) were added. The resulting mixture was heated using microwave reactor at 140 °C for 1 h. After cooling to ambient temperature, the reaction mixture was filtered, and the filtrate was concentrated under reduced pressure. The residue was purified by flash column chromatography (petroleum ether/ethyl acetate = 4:1) to afford the title compound **7** (0.82 g, 76%) as a light yellow foam. ^{1}H NMR (300 MHz, $CDCl_3$): δ 8.88(s, 1H), 8.46(d, J = 5.4 Hz, 1H), 7.91(d, J = 15.6 Hz, 1H), 7.65(s, 1H), 7.04-6.99(m, 1H), 6.89(d, J = 8.1 Hz, 1H), 6.48(d, J = 8.7 Hz, 1H), 6.42-6.37(m, 3H), 5.73(s, 1H), 4.89(m, 1H), 4.28(q, J = 3.9 Hz, 2H), 3.49(m, 2H), 3.17(m, 1H),

2.22(m, 1H), 1.35(t, *J* = 3.9 Hz, 3H), 0.65(m, 3H), -0.27(m, 1H).

Ethyl 3-(2,5-Dichloro-4-((3-(4-cyclopropyl-1,2,3,4-tetrahydroquinoxaline-1-carbonyl)pyridin-4-yl)oxy)phenyl)propanoate (8). To a mixture of **7** (800 mg, 1.48 mmol) and cuprous chloride (147 mg, 1.48 mmol) in methanol (7 mL) and tetrahydrofuran (7 mL), $NaBH_4$ (253 mg, 6.66 mmol) was added at 0 °C, and the resulting mixture was stirred at 0-5 °C for 2 h. Then the reaction was quenched by the addition of water (2 mL). The resulting solid was filtered off, and the filtrate was concentrated under reduced pressure. The residue was diluted with water (10 mL), extracted with ethyl acetate (10 mL × 2). The organic layers were combined, dried over anhydrous magnesium sulfate and evaporated under reduced pressure. The residue was purified by flash column chromatography (petroleum ether/ethyl acetate = 3:1) to give **8** (655 mg, 82%) as a light yellow slurry. ^{1}H NMR (300 MHz, DMSO): δ 8.82(s, 1H), 8.40(d, *J* = 4.2 Hz, 1H), 7.30(s, 1H), 7.03(m, 1H), 6.93(d, *J* = 6.3 Hz, 1H), 6.48(d, *J* = 6.0 Hz, 1H), 6.37(m, 1H), 6.29(d, *J* = 4.2 Hz, 1H), 5.69(s, 1H), 4.89(m, 1H), 4.15(q, *J* = 5.4 Hz, 2H), 3.49(m, 2H), 3.17(m, 1H), 2.99(t, *J* = 5.7 Hz, 2H), 2.61(t, *J* = 5.7 Hz, 2H), 2.25(m, 1H), 1.26(t, *J* = 5.4 Hz, 3H), 0.62(m, 3H), -0.34(m, 1H). ^{13}C NMR (126 MHz, $CDCl_3$) δ 171.57, 163.28, 158.21, 151.81, 151.34, 147.06, 139.80, 136.25, 132.12, 131.08, 126.12, 124.73, 124.16, 123.00, 122.65, 121.88, 115.00, 112.63, 108.78, 66.59, 60.24, 48.37, 39.73, 33.13, 30.42, 27.67, 13.73, 7.18. HRMS (ES^+) calcd for $C_{28}H_{27}Cl_2N_3O_4Na$ $(M+Na)^+$ m/z 562.1276, found 562.1272.

3-(2,5-Dichloro-4-((3-(4-cyclopropyl-1,2,3,4-tetrahydroquinoxaline-1-carbonyl)pyridin-4-yl)oxy)phenyl)propanoic acid (9). To a solution of **8** (639 mg, 1.18 mmol) in 1,4-dioxane (5 mL) and water (5 mL), sodium hydroxide (94.4 mg, 2.36 mmol) was added, and the resulting mixture was stirred at ambient temperature for 3 h. The reaction was evaporated to dryness, and the residue was dissolved in water (10 mL). The pH of the solution was adjusted to 3 with 2N HCl.

The formed precipitate was filtered, washed with cold water, and dried under vacumm to provide the title compound **9** (556 mg, 92%) as a light yellow solid. ^{1}H NMR (300 MHz, DMSO): δ 12.29(s, 1H), 8.77(s, 1H), 8.41(d, J = 3.9 Hz, 1H), 7.59(s, 1H), 6.97(m, 1H), 6.84(m, 1H), 6.53(m, 1H), 6.48(m, 1H), 6.33(m, 1H), 5.54(s, 1H), 4.71(m, 1H), 3.36(m, 2H), 3.07(m, 1H), 2.86(m, 2H), 2.51(m, 1H), 2.16(m, 1H), 0.60(m, 2H), 0.47(m, 1H), -0.44(m, 1H). ^{13}C NMR (126 MHz, $CDCl_3$) δ 175.79, 163.03, 158.56, 151.23, 150.77, 146.91, 139.84, 136.48, 132.20, 131.11, 126.23, 124.61, 124.18, 122.94, 122.83, 121.93, 115.05, 112.70, 108.98, 48.35, 39.81, 33.15, 30.46, 27.71, 7.22. HRMS (ES^+) calcd for $C_{26}H_{24}Cl_2N_3O_4$ $(M+H)^+$ m/z 512.1144, found 512.1141.

General procedure for 10a–c. To a solution of **9** (0.2 mmol) in dichloromethane (5 mL), HATU (0.3 mmol), triethylamine (0.6 mmol) and amino acid ester (0.3 mmol) were added. The resulting mixture was stirred at room temperature overnight. The reaction mixture was diluted with water (10 mL) and extracted with dichloromethane (10 mL). The organic layer was washed with saturated brine, dried over anhydrous magnesium sulfate, and concentrated under reduced pressure. The residue was purified by flash chromatography (petroleum ether/ethyl acetate = 2:1 to 1:1) to give the desired compound.

Ethyl 2-(3-(2,5-Dichloro-4-((3-(4-cyclopropyl-1,2,3,4-tetrahydroquinoxaline-1-carbonyl)pyridin-4-yl)oxy)phenyl)propanamido)acetate (10a). The title compound was obtained from **9** and glycine ethyl ester hydrochloride according to the general procedure in yield of 81%. ^{1}H NMR (300 MHz, $CDCl_3$): δ 8.81(s, 1H), 8.40(m, 1H), 7.31(s, 1H), 7.03(m, 1H), 6.96(m, 1H), 6.48(m, 1H), 6.39-6.31(m, 2H), 5.98(t, J = 4.2 Hz, 1H), 5.72(s, 1H), 4.87(m, 1H), 4.20(q, J = 7.2 Hz, 2H), 4.02(m, 2H), 3.48(m, 2H), 3.20(m, 1H), 3.03(t, J = 7.5 Hz, 2H), 2.53(t, J = 7.5 Hz, 2H), 2.26(m, 1H), 1.28(t, J = 7.2 Hz, 3H), 0.64(m, 3H), -0.28(m, 1H). ^{13}C NMR (126 MHz, $CDCl_3$) δ 172.37, 170.55, 163.19, 158.39, 151.60, 151.08, 146.93, 136.66, 132.05, 131.07,

126.14, 124.69, 124.23, 122.97, 122.68, 121.93, 115.04, 112.64, 108.86, 60.35, 48.36, 39.76, 35.26, 34.37, 33.42, 30.45, 28.20, 13.68, 7.23. HRMS (ES^+) calcd for $C_{30}H_{30}Cl_2N_4O_5Na$ $(M+Na)^+$ m/z 619.1491, found 619.1482.

Ethyl 3-(3-(2,5-Dichloro-4-((3-(4-cyclopropyl-1,2,3,4-tetrahydroquinoxaline-1-carbonyl)pyridin-4-yl)oxy)phenyl)propanamido)propanoate (10b). The title compound was obtained from **9** and β-alanine ethyl ester hydrochloride according to the general procedure in yield of 79%. ^{1}H NMR (300 MHz, $CDCl_3$): δ 8.81(s, 1H), 8.41(d, J = 6.0 Hz, 1H), 7.30(s, 1H), 7.03(m, 1H), 6.96(m, 1H), 6.46(m, 1H), 6.33(m, 1H), 6.31(m, 1H), 6.11(d, J = 6.0 Hz, 1H), 5.73(s, 1H), 4.85(m, 1H), 4.13(q, J = 6.9 Hz, 2H), 3.54-3.49(m, 4H), 3.21(m, 1H), 3.00(t, J = 7.5 Hz, 2H), 2.51(t, J = 6.0 Hz, 2H), 2.44(t, J = 7.5 Hz, 2H), 2.26(m, 1H), 1.25(t, J = 6.9 Hz, 3H), 0.65(m, 3H), -0.27(m, 1H).^{13}C NMR (126 MHz, $CDCl_3$) δ 170.69, 169.46, 163.25, 158.34, 151.68, 151.16, 147.04, 139.81, 136.43, 132.02, 131.21, 126.12, 124.72, 124.32, 122.97, 122.64, 121.97, 115.04, 112.64, 108.87, 61.20, 48.36, 40.87, 39.75, 34.93, 30.45, 28.12, 20.17, 13.64, 7.22. HRMS (ES^+) calcd for $C_{31}H_{32}Cl_2N_4O_5Na$ $(M+Na)^+$ m/z 633.1647, found 633.1651.

Ethyl 2-(3-(2,5-Dichloro-4-((3-(4-cyclopropyl-1,2,3,4-tetrahydroquinoxaline-1-carbonyl)pyridin-4-yl)oxy)phenyl)-N-methylpropanamido)acetate (10c). The title compound was obtained from **9** and ethyl sarcosinate hydrochloride according to the general procedure in yield of 73%. ^{1}H NMR (300 MHz, $CDCl_3$): δ 8.81(s, 1H), 8.40(d, J = 6.0 Hz, 1H), 7.35(s, 1H), 7.04-6.97(m, 2H), 6.49(m, 1H), 6.34(m, 2H), 5.74(s, 1H), 4.85(m, 1H), 4.19(q, J = 6.9 Hz, 2H), 4.12(s, 2H), 3.48(m, 2H), 3.07-2.99(m, 6H), 2.67(m, 2H), 2.26(m, 1H), 1.27(t, J = 6.9 Hz, 3H), 0.64(m, 3H), -0.24(m, 1H). ^{13}C NMR (126 MHz, $CDCl_3$) δ 171.47, 168.74, 163.28, 158.35, 151.68, 151.15, 146.91, 139.80, 137.00, 132.05, 131.42, 126.10, 124.71, 124.30, 122.98, 122.64, 121.89, 115.04, 112.63, 108.83, 60.76, 49.01, 48.35, 39.74, 35.97, 34.58, 32.07, 30.48, 27.81,

13.68, 7.23. HRMS (ES^+) calcd for $C_{31}H_{32}Cl_2N_4O_5Na$ $(M+Na)^+$ m/z 633.1647, found 633.1629.

General procedure for 10d–f. To a solution of **10a–c** (0.1 mmol) in 1, 4-dioxane (3 mL) and water (3 mL), sodium hydroxide (0.2 mmol) was added, and the reaction mixture was stirred at ambient temperature for 2 h. The solution was evaporated to dryness, and the residue was dissolved in water (5 mL). The pH of the solution was adjusted to 3 with 2N HCl. The formed precipitate was filtered, washed with cold water, and dried under vacumm to provide the title compound.

2-(3-(2,5-Dichloro-4-((3-(4-cyclopropyl-1,2,3,4-tetrahydroquinoxaline-1-carbonyl)pyridin-4-yl)oxy)phenyl)propanamido)acetic acid (10d). The title compound was obtained from **10a** according to the general procedure in yield of 89%. ^{1}H NMR (300 MHz, $CDCl_3$): δ 8.77(s, 1H), 8.39(m, 1H), 7.32(s, 1H), 7.02(m, 2H), 6.44(m, 3H), 6.21(s, 1H), 5.74(s, 1H), 4.84(m, 1H), 3.92(s, 2H), 3.47(m, 2H), 3.20(m, 1H), 3.03(m, 2H), 2.54(m, 2H), 2.22(m, 1H), 0.65(m, 3H), -0.25(m, 1H). ^{13}C NMR (126 MHz, $CDCl_3$) δ 174.81, 170.80, 162.89, 158.90, 150.87, 150.25, 146.78, 139.88, 136.89, 132.12, 131.23, 126.31, 124.54, 124.20, 122.87, 121.97, 115.14, 112.81, 109.27, 48.34, 39.90, 35.33, 34.40, 33.27, 30.54, 28.31, 7.27. HRMS (ES^+) calcd for $C_{28}H_{27}Cl_2N_4O_5$ $(M+H)^+$ m/z 569.1359, found 569.1352.

3-(3-(2,5-Dichloro-4-((3-(4-cyclopropyl-1,2,3,4-tetrahydroquinoxaline-1-carbonyl)pyridin-4-yl)oxy)phenyl)propanamido)propanoic acid (10e). The title compound was obtained from **10b** according to the general procedure in yield of 85%. ^{1}H NMR (300 MHz, $CDCl_3$): δ 8.77(s, 1H), 8.41(d, J = 5.4 Hz, 1H), 7.31(s, 1H), 7.02(m, 2H), 6.48(m, 1H), 6.38-6.34(m, 3H), 5.79(s, 1H), 4.77(m, 1H), 3.49(m, 4H), 3.25(m, 1H), 3.01(m, 2H), 2.50-2.45(m, 4H), 2.27(m, 1H), 0.67(m, 3H), -0.20(m, 1H). ^{13}C NMR (126 MHz, $CDCl_3$) δ 171.68, 171.20, 162.49, 159.37, 150.09, 149.39, 146.58, 139.91, 136.95, 132.15, 131.48, 126.41, 124.44, 124.29,

123.11, 122.80, 122.13, 115.16, 112.82, 109.52, 48.30, 41.05, 39.94, 34.98, 30.48, 29.20, 28.32, 7.26. HRMS (ES^+) calcd for $C_{29}H_{29}Cl_2N_4O_5$ $(M+H)^+$ m/z 583.1515, found 583.1519.

2-(3-(2,5-Dichloro-4-((3-(4-cyclopropyl-1,2,3,4-tetrahydroquinoxaline-1-carbonyl)pyridin-4-yl)oxy)phenyl)-N-methylpropanamido)acetic Acid (10f). The title compound was obtained from **10b** according to the general procedure in yield of 90%. ^{1}H NMR (300 MHz, $CDCl_3$): δ 8.81(s, 1H), 8.44(d, J = 5.4 Hz, 1H), 7.38(s, 1H), 7.05-7.01(m, 2H), 6.45(m, 1H), 6.39(m, 2H), 5.77(s, 1H), 4.85(m, 1H), 3.78(s, 2H), 3.48(m, 2H), 3.24(m, 1H), 3.06-3.00(m, 5H), 2.71(m, 2H), 2.27(m, 1H), 0.67(m, 3H), -0.21(m, 1H). ^{13}C NMR (126 MHz, DMSO) δ 171.70, 171.47, 171.22, 163.48, 158.30, 152.75, 151.73, 147.31, 140.51, 138.03, 132.33, 132.03, 126.69, 125.16, 123.98, 123.53, 121.64, 115.35, 113.16, 110.21, 51.24, 49.46, 48.77, 36.41, 34.84, 32.32, 31.90, 27.96, 7.74. HRMS (ES^+) calcd for $C_{29}H_{29}Cl_2N_4O_5$ $(M+H)^+$ m/z 583.1515, found 583.1526.

(E)-isobutyl 4-(2,5-Dichloro-4-((3-(4-cyclopropyl-1,2,3,4-tetrahydroquinoxaline-1-carbonyl)pyridin-4-yl)oxy)phenyl)but-3-enoate (11). Derivative **11** was synthesized according to the procedure for **7** except replacing ethyl acrylate with isobutyl but-3-enoate. ^{1}H NMR (300 MHz, $CDCl_3$): δ 8.83(s, 1H), 8.41(m, 1H), 7.56(s, 1H), 7.02(m, 1H), 6.95(m, 1H), 6.25(d, J = 12.3 Hz, 1H), 6.47(m, 1H), 6.37-6.31(m, 3H), 5.70(s, 1H), 4.89(m, 1H), 3.92(dd, J = 4.8, 2.1Hz, 2H), 3.52(m, 2H), 3.31(dd, J = 2.1, 1.2 Hz, 2H), 3.18(m, 1H), 2.24(m, 1H), 1.96(m, 1H), 0.95(dd, J = 4.8, 1.5 Hz, 6H), 0.65(m, 3H), -0.25(m, 1H).

(E)-4-(2,5-dichloro-4-((3-(4-cyclopropyl-1,2,3,4-tetrahydroquinoxaline-1-carbonyl)pyridin-4-yl)oxy)phenyl)but-3-enoic Acid (12). To a solution of **11** (116 mg, 0.2 mmol) in 1, 4-dioxane (3 mL) and water (3 mL), sodium hydroxide (16 mg, 0.4 mmol) was added, and the reaction mixture was stirred at ambient temperature for 5 h. The reaction was

evaporated to dryness, and the residue was dissolved in water (5 mL). The pH of the solution was adjusted to 3 with 2N HCl. The formed precipitate was filtered, washed with cold water, and dried under vacumm to provide **12** (90 mg, 86%). ^{1}H NMR (300 MHz, $CDCl_3$): δ 8.84(s, 1H), 8.44(d, J = 5.7 Hz, 1H), 7.59(s, 1H), 7.04(m, 1H), 6.97(m, 1H), 6.75(d, J = 15.6 Hz, 1H), 6.48(m, 1H), 6.40-6.32(m, 3H), 5.73(s, 1H), 4.89(m, 1H), 3.48(m, 2H), 3.36(d, J = 7.2 Hz, 2H), 3.21(m, 1H), 2.25(m, 1H), 0.66(m, 3H), -0.20(m, 1H). ^{13}C NMR (126 MHz, $CDCl_3$) δ 174.75, 163.45, 159.09, 151.63, 151.19, 147.83, 140.38, 133.77, 131.44, 128.04, 127.68, 126.77, 126.42, 125.10, 123.40, 122.43, 115.58, 113.24, 109.54, 48.84, 40.34, 38.08, 31.03, 7.78. HRMS (ES^+) calcd for $C_{27}H_{24}Cl_2N_3O_4$ $(M+H)^+$ m/z 524.1144, found 524.1151.

General procedure for 13a–c. To a solution of **9** (0.5 mmol) in dichloromethane (5 mL) was added HATU (0.7 mmol), followed by triethylamine (1.0 mmol) and the corresponding amine-$(CH_2CH_2O)_n$-azide (0.5 mmol). The resulting mixture was stirred at room temperature overnight. The reaction mixture was diluted with water (10 mL) and extracted with dichloromethane (10 mL). The organic layer was washed with saturated brine, dried over anhydrous magnesium sulfate, and concentrated under reduced pressure. The residue was purified by flash chromatography (dichloromethane / methanol = 100:1 to 30:1) to give the desired compound.

N-(2-(2-(2-(2-azidoethoxy)ethoxy)ethoxy)ethyl)-3-(2,5-dichloro-4-((3-(4-cyclopropyl-1,2,3,4-tetrahydroquinoxaline-1-carbonyl)pyridin-4-yl)oxy)phenyl)propanamide (13a). The title compound was obtained from **9** and NH_2-$(CH_2CH_2O)_3$-N_3 according to the general procedure in yield of 78%. ^{1}H NMR (400 MHz, $CDCl_3$) δ 8.81(s, 1H), 8.41(d, J = 5.6 Hz, 1H), 7.23(s, 1H), 7.03(t, J = 8.0 Hz, 1H), 6.95(d, J = 8.0 Hz, 1H), 6.49(d, J = 8.0 Hz, 1H), 6.37(t, J = 8.0 Hz, 1H), 6.30(d, J = 5.6 Hz, 1H), 6.16(m, 1H), 5.72(s, 1H), 4.87(m, 1H), 3.68-3.37(m, 18H),

3.20(m, 1H), 3.02(t, *J* = 7.6 Hz, 2H), 2.47(t, *J* = 7.6 Hz, 2H), 2.25(m, 1H), 0.64(m, 3H), -0.28(m, 1H).

N-(20-azido-3,6,9,12,15,18-hexaoxaicosyl)-3-(2,5-dichloro-4-((3-(4-cyclopropyl-1,2,3,4-tetrahydroquinoxaline-1-carbonyl)pyridin-4-yl)oxy)phenyl)propanamide (13b). The title compound was obtained from **9** and NH_2-$(CH_2CH_2O)_6$-N_3 according to the general procedure in yield of 75%. ^{1}H NMR (400 MHz, $CDCl_3$) δ 8.80(s, 1H), 8.40(d, *J* = 5.6 Hz, 1H), 7.33(s, 1H), 7.03(m, 1H), 6.95(m, 1H), 6.47(m, 2H), 6.37(m, 1H), 6.30(d, *J* = 5.6 Hz, 1H), 5.72(s, 1H), 4.87(m, 1H), 3.68-3.37(m, 30H), 3.21(m, 1H), 3.01(t, *J* = 8.0 Hz, 2H), 2.47(t, *J* = 8.0 Hz, 2H), 2.25(m, 1H), 0.64(m, 3H), -0.28(m, 1H).

N-(26-azido-3,6,9,12,15,18,21,24-octaoxahexacosyl)-3-(2,5-dichloro-4-((3-(4-cyclopropyl-1,2,3,4-tetrahydroquinoxaline-1-carbonyl)pyridin-4-yl)oxy)phenyl)propanamide (13c). The title compound was obtained from **9** and NH_2-$(CH_2CH_2O)_8$-N_3 according to the general procedure in yield of 71%. ^{1}H NMR (400 MHz, $CDCl_3$) δ 8.80(s, 1H), 8.40(d, *J* = 5.8 Hz, 1H), 7.34(d, *J* = 8.0 Hz, 1H), 7.08-6.99(m, 1H), 6.95(d, *J* = 8.1 Hz, 1H), 6.47(d, *J* = 7.8 Hz, 1H), 6.42–6.35(m, 1H), 6.33(d, *J* = 5.6 Hz, 2H), 5.74(s, 1H), 4.85(s, 1H), 3.70–3.59(m, 11H), 3.55(t, *J* = 4.8 Hz, 3H), 3.45(dd, *J* = 9.9, 4.9 Hz, 3H), 3.43–3.36(m, 2H), 3.29–3.14(m, 6H), 3.00(dd, *J* = 15.1, 7.3 Hz, 2H), 2.58–2.41(m, 6H), 2.24(d, *J* = 14.8 Hz, 1H), 1.37(t, *J* = 7.3 Hz, 8H), 0.77-0.44(m, 3H), -0.21(s, 1H).

General procedure for 15a–c. 10% Pd/C (30 mg) was added to a solution of **13a–c** (0.3 mmol) in methanol (8 mL), and the resulting mixture was stirred under an atmosphere of hydrogen (1 atm) at room temperature for 2 h. The reaction mixture was filtered over celite and the filtrate

was evaporated under reduced pressure to give **14a–c**, which were directly used in next step without any further purification. To a solution of **9** (0.3 mmol) in dichloromethane (10 mL) was added HATU (0.42 mmol), triethylamine (0.6 mmol) and **14a-c**. The reaction mixture was stirred at room temperature overnight. The solvent was evaporated and the residue was purified by preparative HPLC (60%–90% methanol/water) to obtain **15a-c.**

N,N'-(((oxybis(ethane-2,1-diyl))bis(oxy))bis(ethane-2,1-diyl))bis(3-(2,5-dichloro-4-((3-(4-cyclopropyl-1,2,3,4-tetrahydroquinoxaline-1-carbonyl)pyridin-4-yl)oxy)phenyl)propanamide) (15a). The title compound was obtained from **13a** according to the general procedure in yield of 63%. ^{1}H NMR (600 MHz, $CDCl_3$) δ 8.82(s, 2H), 8.42(d, J = 5.4 Hz, 2H), 7.34(s, 2H), 7.05(t, J = 7.8 Hz, 2H), 6.97(d, J = 8.4 Hz, 2H), 6.50(d, J = 7.8 Hz, 2H), 6.39(t, J = 7.8 Hz, 2H), 6.31(m, 4H), 5.77(s, 2H), 4.87(m, 2H), 3.64-3.46(m, 20H), 3.24(m, 2H), 3.04(t, J = 7.8 Hz, 4H), 2.50(t, J = 7.8 Hz, 4H), 2.28(m, 2H), 2.17(m, 2H), 0.66(m, 6H), -0.23(m, 2H). ^{13}C NMR (151 MHz, $CDCl_3$) δ 171.17, 163.75, 158.78, 152.33, 151.74, 147.45, 140.31, 137.24, 132.54, 131.59, 126.60, 125.22, 124.72, 123.48, 123.12, 122.40, 115.52, 113.13, 109.26, 70.41, 70.12, 69.95, 48.87, 40.25, 39.29, 35.59, 30.97, 28.71, 7.75. HRMS (ES^+) calcd for $C_{60}H_{63}Cl_4N_8O_9$ $(M+H)^+$ m/z 1179.3472, found 1179.3463.

N,N'-(3,6,9,12,15,18-hexaoxaicosane-1,20-diyl)bis(3-(2,5-dichloro-4-((3-(4-cyclopropyl-1,2,3,4-tetrahydroquinoxaline-1-carbonyl)pyridin-4-yl)oxy)phenyl)propanamide) (15b). The title compound was obtained from **13b** according to the general procedure in yield of 56%. ^{1}H NMR (600 MHz, $CDCl_3$) δ 8.82(s, 2H), 8.43(d, J = 5.4 Hz, 2H), 7.35(s, 2H), 7.04(t, J = 7.8 Hz, 2H), 6.97(d, J = 7.2 Hz, 2H), 6.52(m, 4H), 6.39(t, J = 7.8 Hz, 2H), 6.31(d, J = 6.0 Hz, 2H), 5.77(s, 2H), 4.87(m, 2H), 3.64-3.45(m, 30H), 3.23(m, 2H), 3.04(t, J = 7.8 Hz, 4H), 2.51(t, J = 7.8 Hz, 4H), 2.29(m, 2H), 2.17(m, 2H), 0.67(m, 6H), -0.23(m, 2H). ^{13}C NMR (151 MHz, $CDCl_3$)

δ 171.23, 163.79, 158.78, 152.32, 151.75, 147.38, 140.30, 137.43, 132.65, 131.53, 126.59, 125.22, 124.69, 123.48, 123.10, 122.39, 115.52, 113.14, 109.27, 70.50, 70.48, 70.46, 70.16, 69.88, 48.86, 40.25, 39.31, 35.49, 30.98, 28.66, 7.75. HRMS (ES^+) calcd for $C_{66}H_{75}Cl_4N_8O_{12}$ $(M+H)^+$ m/z 1311.4295, found 1311.4308.

N,N'-(3,6,9,12,15,18,21,24-octaoxahexacosane-1,26-diyl)bis(3-(2,5-dichloro-4-((3-(4-cyclopropyl-1,2,3,4-tetrahydroquinoxaline-1-carbonyl)pyridin-4-yl)oxy)phenyl)propanamide) (15c). The title compound was obtained from **13c** according to the general procedure in yield of 49%. ^1H NMR (600 MHz, $CDCl_3$) δ 8.82(s, 2H), 8.42(d, J = 6.0 Hz, 2H), 7.35(s, 2H), 7.04(t, J = 7.8 Hz, 2H), 6.97(d, J = 8.4 Hz, 2H), 6.50(d, J = 7.8 Hz, 2H), 6.44(m, 2H), 6.39(t, J = 7.8 Hz, 2H), 6.32(d, J = 6.0 Hz, 2H), 5.76(s, 2H), 4.87(m, 2H), 3.68-3.46(m, 38H), 3.23(m, 2H), 3.03(t, J = 7.8 Hz, 4H), 2.49(t, J = 7.8 Hz, 4H), 2.29-2.24(m, 4H), 0.65(m, 6H), -0.24(m, 2H). ^{13}C NMR (151 MHz, $CDCl_3$) δ 171.16, 163.79, 158.76, 152.32, 151.76, 147.38, 140.30, 137.41, 132.57, 131.54, 126.59, 125.21, 124.68, 123.47, 123.10, 122.36, 115.51, 113.13, 109.28, 70.53, 70.51, 70.49, 70.18, 69.85, 48.86, 40.24, 39.30, 35.50, 30.97, 28.65, 7.75. HRMS (ES^+) calcd for $C_{70}H_{83}Cl_4N_8O_{14}$ $(M+H)^+$ m/z 1399.4783, found 1399.4778.

ASSOCIATED CONTENT

Supporting Information

HPLC purity for all the final compounds and experimental methods for LC/MS/MS are is available free of charge via the Internet at http://pubs.acs.org.

AUTHOR INFORMATION

Corresponding Author

*For Ying Leng : Phone: 86-21-50806059. E-mail: yleng@mail.shcnc.ac.cn.

For Jianhua Shen : Phone: 86-21-20231969. E-mail: jhshen@mail.shcnc.ac.cn.

Author Contributions

†These authors contributed equally to this work.

ACKNOWLEDGEMENT

This work was financially supported by grant from "National Science and Technology Major Project-Key New Drug Creation and Manufacturing program, China" (2012ZX09103101-049) and National Nature Science Foundation of China (Grant 81202571).

ABBREVIATIONS USED

TGR5, Takeda G-protein-coupled receptor 5; T2DM, type 2 diabetes mellitus; EC_{50}, effective concentration for 50% inhibition; BA, bile acids; CA, cholic acid; LCA, lithocholic acid; TLCA, taurolithocholic acid; ASBT, apical sodium-dependent bile acid transporter; GI, gastrointestinal; hTGR5, human TGR5; mTGR5, mouse TGR5; PSA, polar surface area; ICR, Institute of Cancer Research; OGTT, oral glucose tolerance test; AUC, the area under curve; GLP-1, glucagons-like peptide; PEG, polyethylene glycol; DMF, *N,N*-dimethylformamide; THF, tetrahydrofuran; DCM, dichloromethane; CMC, carboxymethyl cellulose; HATU, 1-[bis(dimethylamino)methylene]-1*H*-1,2,3-triazolo[4,5-b]pyridinium 3-oxid hexafluorophosphate; DPP-4, dipeptidyl peptidase-4; EDTA, ethylenediaminetetraacetic acid; PK, pharmacokinetics; SD rats, Sprague–Dawley rats, DMEM, Dulbecco's Modified Eagle Medium; FBS, Fetal Bovine Serum.

REFERENCES

1. Maruyama, T.; Miyamoto, Y.; Nakamura, T.; Tamai, Y.; Okada, H.; Sugiyama, E.; Itadani, H.; Tanaka, K. Identification of membrane-type receptor for bile acids (M-BAR). *Biochem. Biophys. Res. Commun.* **2002**, *298*, 714–719.

2. Katsuma, S.; Hirasawa, A.; Tsujimoto, G. Bile acids promote glucagon-like peptide-1 secretion through TGR5 in a murine enteroendocrine cell line STC-1. *Biochem. Biophys. Res. Commun.* **2005**, *329*, 386–390.

3. Stoffers, D. A.; Kieffer, T. J.; Hussain, M. A.; Drucker, D. J.; Bonner-Weir, S.; Habener, J. F.; Egan, J. M. Insulinotropic GLP-1 peptide agonists stimulate expression of homeodomain protein IDX-1 and increase islet size in mouse pancreas. *Diabetes*. **2000**, *49*, 741–748.

4. Wettergren, A.; Wojdemann, M.; Holst, J. J. The inhibitory effect of glucagon-like peptide-1 (7 36) amide on antral motility is antagonized by its N-terminally truncated primary metabolite GLP-1 (9 36) amide. *Peptides*. **1998**, *19*, 877–882.

5. Watanabe, M.; Houten, S. M.; Mataki, C.; Christoffolete, M. A.; Kim, B. W.; Sato, H.; Messaddeq, N.; Harney, J. W.; Ezaki, O.; Kodama, T.; Schoonjans, K.; Bianco, A. C.; Auwerx, J. Bile acids induce energy expenditure by promoting intracellular thyroid hormone activation. *Nature.* **2006**, *439*, 484–489.

6. Maruyama, T.; Tanaka, K.; Suzuki, J.; Miyoshi, H.; Harada, N.; Nakamura, T.; Miyamoto, Y.; Kanatani, A.; Tamai, Y. Targeted disruption of G protein-coupled bile acid receptor 1 (Gpbar1/M-Bar) in mice. *J. Endocrinol.* **2006**, *191*, 197–205.

7. Chen, X.; Lou, G.; Meng, Z.; Huang, W. TGR5: a novel target for weight maintenance

and glucose metabolism. *Exp. Diabetes. Res.* **2011**, 853501.

8. Pols, T. W.; Noriega, L. G.; Nomura, M.; Auwerx, J.; Schoonjans, K. The bile acid membrane receptor TGR5 as an emerging target in metabolism and inflammation. *J. Hepatol.* **2011**, *54*, 1263–1272.

9. Zhong, M. TGR5 as a therapeutic target for treating obesity. *Curr. Top. Med. Chem.* **2010**, *10*, 386–396.

10. Kawamata, Y.; Fujii, R.; Hosoya, M.; Harada, M.; Yoshida, H.; Miwa, M.; Fukusumi, S.; Habata, Y.; Itoh, T.; Shintani, Y.; Hinuma, S.; Fujisawa, Y.; Fujino, M. A G protein-coupled receptor responsive to bile acids. *J. Biol. Chem.* **2003**, *278*, 9435–9440.

11. Vassileva, G.; Golovko, A.; Markowitz, L.; Abbondanzo, S. J.; Zeng, M.; Yang, S.; Hoos, L.; Tetzloff, G.; Levitan, D.; Murgolo, N. J.; Keane, K.; Davis, Jr, H. R.; Hedrick, J.; Gustafson, E. L. Targeted deletion of Gpbar1 protects mice from cholesterol gallstone formation. *Biochem. J.* **2006**, *398*, 423–430.

12. Watanabe, M.; Houten, S. M.; Mataki, C.; Christoffolete, M. A.; Kim, B. W.; Sato, H.; Messaddeq, N.; Harney, J. W.; Ezaki, O.; Kodama, T.; Schoonjans, K.; Bianco, A. C.; Auwerx, J. Bile acids induce energy expenditure by promoting intracellular thyroid hormone activation. *Nature.* **2006**, *439*, 484–489.

13. Li, T.; Holmstrom, S. R.; Kir, S.; Umetani, M.; Schmidt, D. R.; Kliewer, S. A.; Mangelsdorf, D. J. The G protein-coupled bile acid receptor, TGR5, stimulates gallbladder filling. *Mol. Endocrinol.* **2011**, *25*, 1066–1071.

14. Fryer, R. M.; Ng, K. J.; Nodop Mazurek, S. G.; Patnaude, L.; Skow, D. J.; Muthukumarana, A.; Gilpin, K. E.; Dinallo, R. M.; Kuzmich, D.; Lord, J.; Sanyal, S.; Yu, H.; Harcken, C.; Cerny, M. A.; Hickey, E. R.; Modis, L. K. G protein–coupled bile acid receptor 1 (GPBAR1) stimulation mediates arterial vasodilation through a $K_{Ca}1.1$ (BK_{Ca})–dependent mechanism. *J. Pharmacol. Exp. Ther.* **2014**, *348*, 421-431.

15. Piotrowski, D. W.; Futatsugi, K.; Warmus, J. S.; Orr, S. T. M.; Freeman-Cook, K. D.; Londregan, A. T.; Wei, L.; Jennings, S. M.; Herr, M.; Coffey, S. B.; Jiao, W.; Storer, G.; Hepworth, D.; Wang, J.; Lavergne, S. Y.; Chin, J. E.; Hadcock, J. R.; Brenner, M. B.; Wolford, A. C.; Janssen, A. M.; Roush, N. S.; Buxton, J.; Hinchey, T.; Kalgutkar, A. S.; Sharma, R.; Flynn, D. A. Identification of tetrahydropyrido[4,3-*d*]pyrimidine amides as a new class of orally bioavailable TGR5 agonists. ACS Med. Chem. Lett. **2012**, *4*, 63-68.

16. Pellicciari, R.; Gioiello, A.; Macchiarulo, A.; Thomas, C.; Rosatelli, E.; Natalini, B.; Sardella, R.; Pruzanski, M.; Roda, A.; Pastorini, E.; Schoonjans, K.; Auwerx, J. Discovery of 6α-ethyl-23(S)-methylcholic acid (S-EMCA, INT-777) as a potent and selective agonist for the TGR5 receptor, a novel target for diabesity. *J. Med. Chem.* **2009**, *52*, 7958–7961.

17. Budzik, B. W.; Evans, K. A.; Wisnoski, D. D.; Jin, J.; Rivero, R. A.; Szewczyk, G. R.; Jayawickreme, C.; Moncol, D. L.; Yu, H. Synthesis and structure–activity relationships of a series of 3-aryl-4-isoxazolecarboxamides as a new class of TGR5 agonists. *Bioorg. Med. Chem. Lett.* **2010**, *20*, 1363–1367.

18. Herbert, M. R.; Siegel, D. L.; Staszewski, L.; Cayanan, C.; Banerjee, U.; Dhamija, S.; Anderson, J.; Fan, A.; Wang, L.; Rix, P.; Shiau, A. K.; Rao, T. S.; Noble, S. A.; Heyman, R. A.; Bischoff, E.; Guha, M.; Kabakibi, A.; Pinkerton, A. B. Synthesis and SAR of 2-aryl-3-

aminomethylquinolines as agonists of the bile acid receptor TGR5. *Bioorg. Med. Chem. Lett.* **2010**, *20*, 5718–5721.

19. Evans, K. A.; Budzik, B. W.; Ross, S. A.; Wisnoski, D. D.; Jin, J.; Rivero, R. A.; Vimal, M.; Szewczyk, G. R.; Jayawickreme, C.; Moncol, D. L.; Rimele, T. J.; Armour, S. L.; Weaver, S. P.; Griffin, R. J.; Tadepalli, S. M.; Jeune, M. R.; Shearer, T. W.; Chen, Z. B.; Chen, L.; Anderson, D. L.; Becherer, J. D.; De Los Frailes, M.; Colilla, F. J. Discovery of 3-aryl-4-isoxazolecarboxamides as TGR5 receptor agonists. *J. Med. Chem.* **2009**, *52*, 7962–7965.

20. Bissantz, C.; Dehmlow, H.; Martin, R. E.; Obst, S. U.; Richter, H.; Ullmer, C. Preparation of novel phenyl amide or pyridyl amide derivatives as GPBAR1 agonists for treating type II diabetes. US20100105906A1, **2010**.

21. Maruyama, M. Therapeutic agent for irritable bowel syndrome containing TGR5 receptor agonists. WO2010016552A1, **2010**.

22. Phillips, D. P.; Gao, W.; Yang, Y.; Zhang, G.; Lerario, I. K.; Lau, T. L.; Jiang, J.; Wang, X.; Nguyen, D. G.; Bhat, B. G.; Trotter, C.; Sullivan, H.; Welzel, G.; Landry, J.; Chen, Y.; Joseph, S. B.; Li, C.; Gordon, W. P.; Richmond, W.; Johnson, K.; Bretz, A.; Bursulaya, B.; Pan, S.; McNamara, P.; Seidel, H. M. Discovery of trifluoromethyl(pyrimidin-2-yl)azetidine-2-carboxamides as potent, orally bioavailable TGR5 (GPBAR1) agonists: structure–activity relationships, lead optimization, and chronic in vivo efficacy. *J. Med. Chem.* **2014**, *57*, 3263.

23. Zou, Q.; Duan, H.; Ning, M.; Liu, J.; Feng, Y.; Zhang, L.; Zhu, J.; Leng, Y.; Shen, J. 4-Benzofuranyloxynicotinamide derivatives are novel potent and orally available TGR5 agonists. *Eur. J. Med. Chem.* **2014**, *82*, 1-15.

24. Duan, H.; Ning, M.; Chen, X.; Zou, Q.; Zhang, L.; Feng, Y.; Zhang, L.; Leng, Y.; Shen, J. Design, synthesis and anti-diabetic activity of 4-phenoxynicotinamide and 4-phenoxypyrimidine-5-carboxamide derivatives as potent and orally efficacious TGR5 agonists. *J. Med. Chem.* **2012**, *55*, 10475−10489.

25. (a) Stoffers, D.; Kieffer, T.; Hussain, M. A.; Drucker, D. J.; Bonner-Weir, S.; Habener, J.; Egan, J. Insulinotropic GLP-1 peptide agonists stimulate expression of homeodomain protein IDX-1 and increase islet size in mouse pancreas. *Diabetes.* **2000**, *49*, 741–748. (b) Wettergren, A.; Wojdemann, M.; Holst, J. J. The inhibitory effect of glucagon-like peptide-1 (7 36) amide on antral motility is antagonized by its N-terminally truncated primary metabolite GLP-1 (9 36) amide. *Peptides.* **1998**, *19*, 877–882.

26. Harach, T.; Pols, T. W.; Nomura, M.; Maida, A.; Watanabe, M.; Auwerx, J.; Schoonjans, K. TGR5 potentiates GLP-1 secretion in response to anionic exchange resins. *Sci. Rep.* **2012**, *2*, 430.

27. Charmot, D. Non-systemic drugs: a critical review. *Curr. Pharm. Design.* **2012**, *18*, 1434–1445.

28. Lembcke, B.; Löser, C.; Fölsch, U. R.; Wöhler, J.; Creutzfeldt, W. Adaptive responses to pharmacological inhibition of small intestinal a-glucosidases in the rat. *Gut*. **1987**, *28*, SI, 181–187.

29. Wu, Y.; Aquino, C. J.; Cowan, D. J.; Anderson, D. L.; Ambroso, J. L.; Bishop, M. J.; Boros, E. E.; Chen, L.; Cunningham, A.; Dobbins, R. L.; Feldman, P. L.; Harston, L. T.; Kaldor, I. W.; Klein, R.; Liang, X.; McIntyre, M. S.; Merrill, C. L.; Patterson, K. M.; Prescott,

J. S.; Ray, J. S.; Roller, S. G.; Yao, X.; Young, A.; Yuen, J.; Collins, J. L. Discovery of a highly potent, nonabsorbable apical sodium-dependent bile acid transporter inhibitor (GSK2330672) for treatment of type 2 diabetes. *J. Med. Chem.* **2013**, *56*, 5094−5114.

30. (a) Venkataiah, B; Clayton, B. B.; Jackline, D.; Brenton, F.; Nadia, H.; Sarah, H.; Raju, M. Michael. M.; Benjamin, P. TGR5 agonists. WO2011071565A1, **2010**. (b) Brenton, F.; Raju, M. TGR5 agonists: imidazole and triazole compounds containing a quaternary nitrogen. WO2014100021, **2013**. (c) Brenton, F.; Raju, M. TGR5 agonists having an imidazole or triazole core with subtituent having a quaternary nitrogen. WO2014100025A1, **2013**.

31. Lewis, J. G.; Reich. N.; Chen. T.; Jacobs. J. W.; Charmot. D.; Navre. M.; Finn. P.; Carreras. C.; Spencer. A. Non-systemic TGR5 agonists. WO2013096771A1, **2012**.

32. Lipinski, C. A.; Lombardo, F.; Dominy, B. W.; Feeney, P. J. Experimental and computational approaches to estimate solubility and permeability in drug discovery and development settings. *Adv. Drug. Deliv. Rev.* **2001**, *46*, 3–26.

33. Egan, W. J.; Merz, K. M., Jr.; Baldwin, J. J. Prediction of drug absorption using multivariate statistics. *J. Med. Chem.* **2000**, *43*, 3867−3877.

34. Veber, D. F.; Johnson, S. R.; Cheng, H.; Smith, B. R.; Ward, K. W.; Kopple, K. D. Molecular properties that influence the oral bioavailability of drug candidates. *J. Med. Chem.* **2002**, *45*, 2615–2623.

35. Palm, K.; Stenberg, P.; Luthman, K.; Artursson, P. Polar molecular surface properties predict the intestinal absorption of drugs in humans. *Pharm. Res.* **1997**, *14*, 568–571.

36. Eckhardt, M.; Langkopf, E.; Mark, M.; Tadayyon, M.; Thomas, L.; Nar, H.; Pfrengle, W.; Guth, B.; Lotz, R.; Sieger, P.; Fuchs, H.; Himmelsbach, F. 8-(3-(R)-aminopiperidin-1-yl)-7-but-2-ynyl-3-methyl-1-(4-methyl-quinazolin-2-ylmethyl)-3,7-dihydropurine-2,6-dione (BI1356), a highly potent, selective, long-acting, and orally bioavailable DPP-4 inhibitor for the treatment of type 2 diabetes. *J. Med. Chem.* **2007**, *50*, 6450−6453.

37. Simpson, A. K.; Ward, P. S.; Wong, K. Y.; Collord, G. J.; Habib, A. M.; Reimann, F.; Gribble, F. M. Cyclic AMP triggers glucagon-like peptide-1 secretion from the GLUTag enteroendocrine cell line. *Diabetologia.* **2007**, *50*, 2181–2189.

38. Anini, Y.; Brubaker, P. L. Role of leptin in the regulation of glucagon-like peptide-1 secretion. *Diabetes*. **2003**, *52*, 252–259.

Table of Contents Graphic

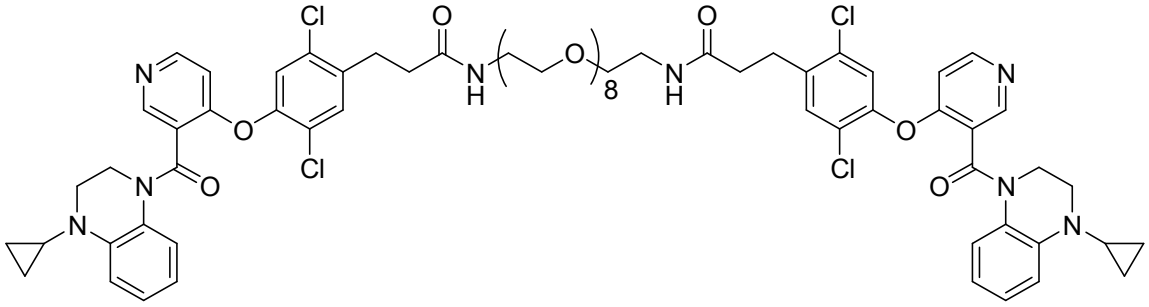

MW = 1401, PSA = 223 Å^2

hTGR5 EC_{50} = 25 nM, mTGR5 EC_{50} = 12 nM

Low permeability and systemic exposure

30% Reduction in $(AUC)_{0\text{-}120\ min}$ during OGTT in ICR mice